THE LIPID WORLD THEORY AND RNA POLYMERIZATION

METABOLISM FIRST OR GENES FIRST?

INVESTIGATION OF THEORIES ABOUT

THE ORIGIN OF LIFE

By
MENG WU, B.Sc., M.Sc.

A Thesis
Submitted to the School of Graduate Studies
in Partial Fulfilment of the Requirement
for the Degree
Master of Science

McMaster University

MASTER OF SCIENCE (2008) McMaster University
(Physics and Astronomy) Hamilton, Ontario

TITLE: Metabolism First or Genes First? Investigation of Theories about the Origin of Life

AUTHOR: Meng Wu, B.Sc., M.Sc.

SUPERVISOR: Dr. Paul G. Higgs

NUMBER OF PAGES: xii, 71

Abstract

Popular theories about the origin of life can be classified to two classes: metabolism first or genes first. As a metabolism first theory, the lipid world theory, in which non-covalent assemblies of lipids, such as micelles and vesicles store information in the form of a non-random molecular composition, has been proposed to investigate the possibility of inheritance without genes. Our models assume that interaction occurs between nearest neighbour molecules only, and account for spatial segregation of molecules of different types within the assembly. We also draw a distinction between a self-assembly model, in which the composition is determined by mutually favourable interaction energies between the molecules, and a catalytic model, in which the composition is determined by mutually favourable catalysis. We show that compositional inheritance occurs in both models, although the self-assembly case seems more relevant if the molecules are simple lipids. In the case where the assemblies are composed of just two types of molecules, there is a strong analogy with the classic two-allele Moran model from population genetics. This highlights the parallel between compositional inheritance and genetic inheritance. We also investigated the polymerization reactions which may bridge the gap between simple organic molecules and the beginning of the RNA world, which belongs to the class of genes first theories. We found that different from normal chemical systems, catalysts for the polymerization system can shift the equilibrium toward longer polymers. Together with RNA's potential as catalyst, the RNA

polymerization system may form a feedback loop which makes the formation of functional RNA molecules easier, and come more close to the beginning of RNA world.

Acknowledgements

I would like to thank my supervisor Dr. Paul Higgs for all his invaluable help and directions.

I would like to thanks Nicholas Waglechner, Wenqi Ran, Wenli Jia, Kai Cai, Jiajia Zhou and Jianfeng Li for their inspiring discussions and suggestion for the research, and also for their encouragement in life.

I would also like to take this opportunity to thank my family for their support.

dedicated to my family

Table of Contents

List of Figures

List of Tables

Chapter 1

Introduction to Theories and Models for the Origin of Life

1.1 Where, When, and How did Life Originate?

From whales to bacteria, from birds to plants, there is a great diversity of forms of life living on earth. Centuries of biological studies show that all forms of life evolve from a common ancestor through inheritable mutation selected by survival, competition, and adaptation to environmental pressure. After understanding the mechanism of evolution from the common ancestor, more questions arose: where and when is this common ancestor from? How were simple organic molecules such as amino acids and nucleotides formed? How did long biopolymers form from monomers? How did metabolism and genetic system form from a community of biopolymers? How did a modern form of cellular life originate from combination of all these subsystems? Any of the above questions are of great importance to our essential knowledge of life. In this thesis, I tried to review different answers to these question and tried to answer a few of them by myself.

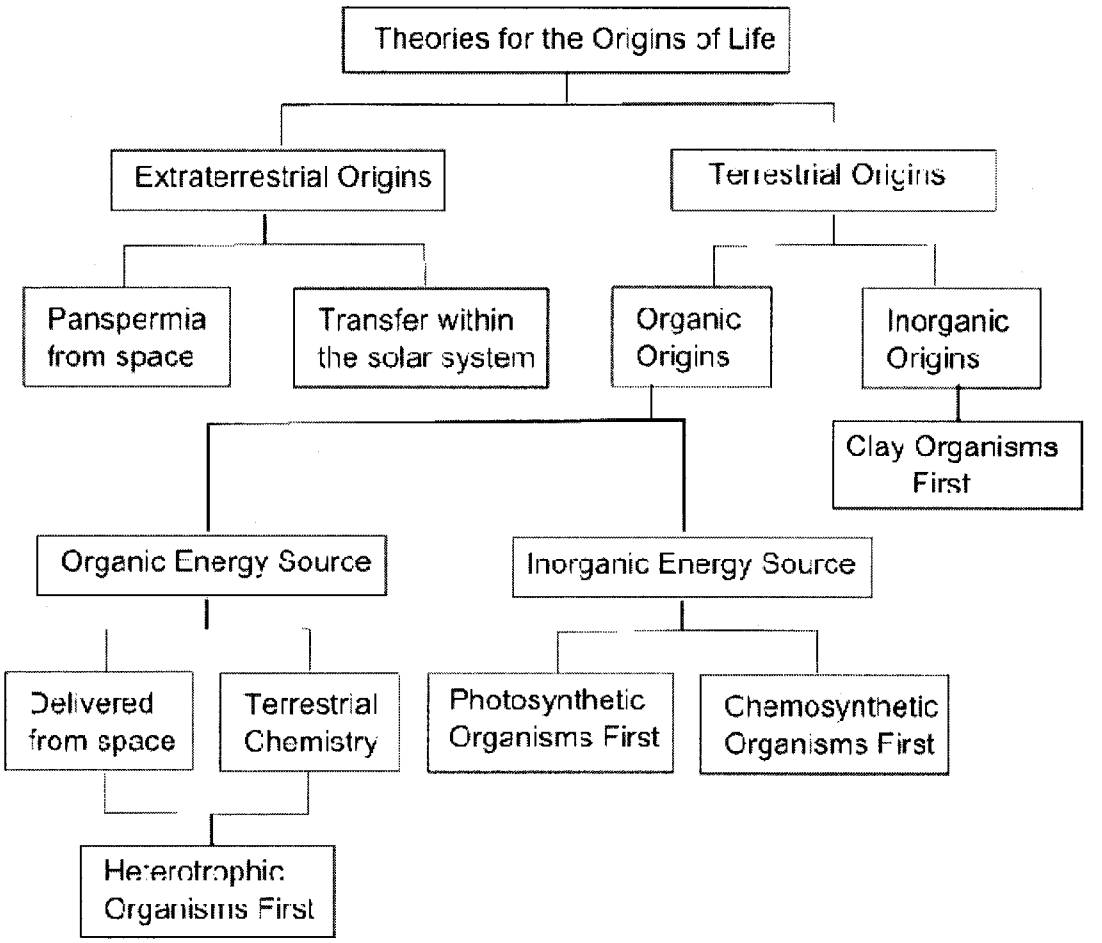

Fig 1.1: Popular theories about the origin of life. Reproduced from Fig 9.1 in Lunine (2005).

Two classes of theory explain where life came from: Panspermia, *i.e.* out of earth (Hoyle and Wickramasinghe, 1999), or from earth. There are two lines of evidence supporting the Panspermia theory. One is the narrow time window between the cool down of the Earth's surface and the first life fossil. The other is that some forms of life such as extremophiles can tolerate very wide range of environment, possibly even millions of years of space travel and entry impact (Tepfer and Leach 2006). However, a crucial criteria for scientific theory is testability. We can verify the possibility of inter-planetary or even inter-galactic travel for life (Clark 2001). But it's beyond our current reach to

investigate why and how life originates at other planet or galaxy. Hence we will focus on abiogenesis theory on earth.

Based on isotopic analysis on the oldest rocks on earth and meteorites, it is thought that the earth formed at 4.5 billion years ago (Dalrymple 1991). However, only after the end of the late heavy bombardment at around 3.9 billion years ago, during which intense stream of huge meteorites hit the earth and melt its surface from time to time, it is possible for life to evolve uninterruptedly (Morbidelli 2007). The earliest isotopic evidence for life is found to be 3.8 billion years ago, while the earliest microfossil from 3.5 billions of years ago, which already has complex structures (Mojzsis 1996; Schopf 1993). Hence the time window for the origin of life must be no later than 3.8 billion years ago, and may be in the decline of the late heavy bombardment.

For the origin of life on earth, building block of life such as amino acid and nucleotides must be synthesized abiotically. Produced from nuclear reaction in stars, important elements for life such as hydrogen, carbon, oxygen and nitrogen are widely available in the universe, and can form simple molecules in the space. This type of reducing molecular gas is presumed to constitute the primordial atmosphere of the earth This environment is assumed by Oparin and Haldane to be favourable for the formation of organic molecules (Oparin, 1924; Haldane, 1929). Based on this hypothesis, Miller carried out the famous Miller-Urey spark discharge experiments (Miller 1953). In these experiments, the mixed gas of hydrogen, ammonia, methane and water was heated and cycled through spark firing chamber which simulated lighting in the hypothetical primordial atmosphere. After only one week of continuous operation, several types of

amino acid are formed, along with sugars, lipids and some bases for nucleotides. Following inspired experiments proved that as long as the gas is reducing and with balanced elements, different chemical composition and energy input method such as ultraviolet light can always produce these basic building blocks for life.

However, the reducing primordial atmosphere hypothesis was challenged later. Due to small size of earth and heavy meteorite bombardments in the formation period of solar system, light elements of the primordial atmosphere such as hydrogen may be depleted, which fact will make the atmosphere more oxidizing. On the other hand, widely existence of Fe^{2+} mineral sediment before the era of photosynthesis proved that the atmosphere won't be totally oxidizing either. It has also been shown that not-so-reducing atmosphere can also produce organic molecules albeit less efficient (Stribling and Miller, 1987).

Aside from the lighting method, there are also other ways to produce simple organic molecules. One important source is the hydrothermal vent in the deep ocean created by volcano activities. Independent of the redox state of atmosphere, reducing gas has been emitting from these hydrothermal vents since the formation of earth. With the help of thermal energy, basic organic molecules such as amino acid and lipids are ready to form in this reducing environment.

One of the major obstacles for prebiotic synthesis is the nucleotide, which is made up of a phosphate, a sugar and a nucleobase. Only phosphate is widely available in nature. Both sugars and nucleobases require high concentration of their respective precursors in reducing environments for reasonable yield. It's even more difficult to stick these three

parts together correctly to produce nucleotides. Considering possible linkage between phosphate, sugar and base, there is only one correct configuration out of hundreds of wrong ones. And the polymerization between those nucleotides without purification, which is also a very complex process, is nearly impossible to make perfect long RNA. At present, it has not been possible to synthesize RNA in a prebiotically plausible way in the laboratory, and this has led some chemists to propose alternative nucleic acids with simplified backbones, such as TNA or PNA (see Fig. 1.2), which may be easier to form (Orgel 2004).

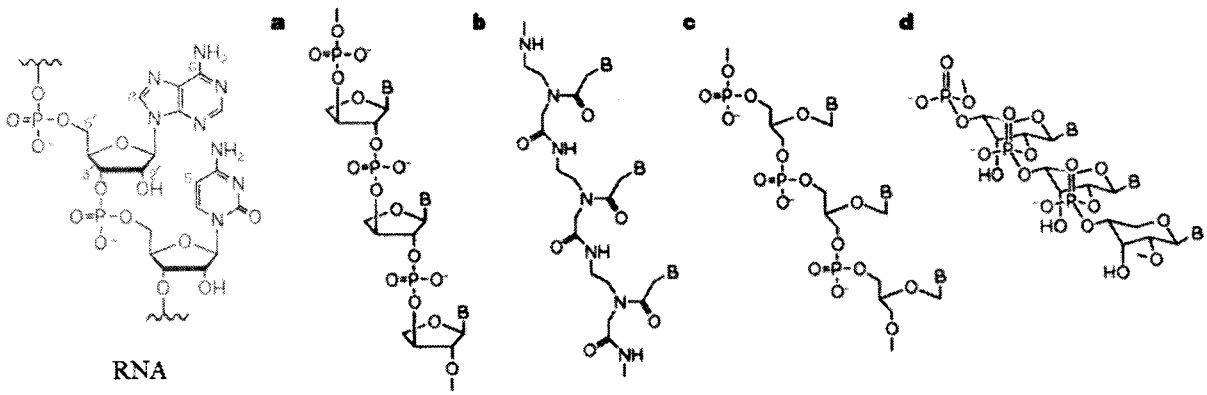

Fig 1.2 Molecular structure of RNA and a. Threose Nucleic Acid (TNA); b. Peptide Nucleic Acid (PNA); c. Glycerol derived nucleic acid; d. Pyranosyl RNA (Joyce, 2002)

1.2 The RNA World

With the formation of all these building blocks, life itself can start to emerge. All cellular life has three essential components (Ganti, 1979; Szathmary et al. 2005). A genetic system is required to store information and to pass that information on in a heritable way. A metabolic system is required to synthesize the necessary molecules and

generate energy in a form that is usable by the organism. A boundary system (such as a cell membrane) is required to distinguish individuals from each other and the environment. Only when we have distinct individuals can multiplication, competition and evolution occur. However, the simplest conceivable cell possessing all three components is already rather complex; therefore when considering the origin of life, it is natural to ask whether something simpler could have existed that did not possess all three.

One approach to the origin of life focuses on the RNA world theory. Playing its majority roles as information molecules in modern cell, RNA is also found to be capable of versatile catalytic functions as ribozyme. Hence, it is likely that there was an RNA world period in the early history of life on earth in which RNA was the informational polymer and also the key catalytic molecule (Gilbert, 1986; Jeffares et al. 1998; Joyce, 2002; Orgel, 2004). The main evidence for this is that the sequences of proteins in modern cells are encoded in mRNAs, that rRNAs are the main functional component of the ribosome, and that tRNAs enable translation to occur via the codon-anticodon interactions that define the genetic code. Several other types of RNA that may be relics of the RNA world are also known. For example, the tRNA-like substrate cleaving RNase P holoenzyme, which composed of RNA and protein, may be a relic of transition from pure RNA ribozyme to RNP world (Liu and Altman 1994). Involvement of tRNA and amino acid complex in some intermediate metabolism may indicate the similar transition (Schon 1986; Roberts 1968; Rogers and Soll 1995). Many snorposomes, which are small nucleolar RNA responsible for ribosome mutation, are encoded within introns of proteins (Maxwell and Fournier 1995). And their formation dependence on splicesome, which is a

complex of RNA and protein removing introns from mRNA, instead of enzyme, may hint that they are relic from pre-enzyme world, i.e., the RNA world (Kiss and Philiowicz, 1995). We therefore envisage an RNA world in which there were RNA-based cells containing a fairly diverse set of functional RNA molecules. The origin of translation and the genetic code would have occurred in such RNA-based cells (Higgs & Pudritz, 2007).

Cells in a late-stage RNA world would have possessed all three of the essential components. What preceded this stage? A stronger version of the RNA world hypothesis is that life originated in the form of self-replicating RNA molecules. Considerable progress has been made in the in vitro synthesis of polymerase ribozymes that are able to synthesize oligomers in a template-directed manner (Bartel and Unrau, 1999; Johnston et al. 2001; Zaher and Unrau, 2007).

However, this kind of in vitro evolution for polymerase ribozymes is very hard to happen spontaneously. Firstly, in vitro selection and amplification are all carried out with the help of highly efficient enzyme or ribozyme which may not be available at the beginning of life (Romero-Lopez and Diaz-Gonzalez, 2007). Secondly, all known template-directed polymerase ribozymes are of the length of hundreds of nucleotides (100~200). Without pre-existing template-directed polymerase ribozymes, the formation of long polynucleotides with specified sequence by random extension will be extremely inefficient. The amplification of this type of ribozyme requires at least two molecules, one as replicator and another as template. Thirdly, even the best template-directed polymerase ribozymes currently known can only extend the prime by around 20 nucleotides (Zaher and Unrau, 2007). Together with the instability of RNA and the

availability of activated nucleotides in prebiotic environment, the chance for the spontaneous emergence of template-directed polymerase ribozymes is quite close to zero. Hence there must be some other steps before the template-directed polymerase ribozymes.

With water as by product, RNA polymerization can be made favourable by either inputting energy or removing the water. The first approach is widely used in the form of activated monomers such as imidazole esters of nucleotides (Inoue and Orgel 1983; Orgel 1998). Rajamani et al took the second approach by mixing lipids with nucleotides and treating them through wet-dry cycles (Rajamani et al, 2008). Enclosed by lipid vesicles, water can easily escape from this microenvironment, which drives the reaction towards polymerization. The final product as RNA-like polymers in the length of 25-100 nucleotides also proves this approach is possible.

Similarly, neither enzymes nor ribozymes are the only possible catalysts for RNA polymerization. By continuously supplying activated nucleotides to montmorillonite, which is a type of layered clay absorbing polymers, Ferris et al proved that polynucleotides longer than 50 monomers can be formed (Ferris 1996, 2002). Divalent cations can also catalyze the condensation of activated nucleotides (Sleeper & Orgel, 1979). On the other hand, a 31-mer polynucleotide, with a effective structure of 7 nucleotides can already catalyze the cleavage of itself (Kazakov and Altman 1992, Kazakov 1996). Hence, among the polynucleotides produced by inorganic catalyst, polymerase ribozyme may emerge that are better catalysts than the original inorganic catalysts.

By definition, a catalyst changes the forward and backward reaction rate simultaneously and does not change the equilibrium concentration of reactants and products. But in a chemical reaction network, things may be different. Due to the concentration difference, the forward rate will faster than backward rate at the beginning. The addition of catalyst to this system can amplify the difference between forward rate and backward rate, and may channel more material into reactions in which products of the first reactions act as reactant. In the case of nucleotides polymerization, it is possible that an increment of polymerization efficiency will shift the equilibrium towards longer polymers, among which may emerge even higher efficiency polymerization catalysts. When the polymer length reaches over 100 nucleotides, the emergence of template directed polymerase ribozyme is possible. If it is true, then the gap between pre-RNA world and RNA world can be bridged.

1.3 Autocatalytic Sets

Instead of using information-carrying polymers as an initial step, there is another approach for origin of life. Several authors have proposed 'metabolism first' theories in which a self-sustaining network of chemical reactions arises in absence of informational polymers or cells. It is presumed that a 'food' set of small molecules is present in the environment and is maintained at a high concentration. These molecules may react together in many ways to produce a huge variety of larger molecules. Spontaneous reactions are assumed to be slow, but some of the larger molecules have the ability to catalyze some of the possible reactions and make them proceed much faster than the

spontaneous rate. An autocatalytic set of the larger molecules may arise, i.e. each molecule in the autocatalytic set can be formed by reactions involving the food set and other members of the autocatalytic set, and each formation reaction is catalyzed by another molecule in the set. Kauffman (1986) considered a model in which the possible molecules are copolymers made from a small number of monomeric units, and the possible reactions are ligation and hydrolysis of these copolymers. The food set is the set of oligomers of length shorter than some initial length L. Autocatalytic subsets of long polymers are found to arise frequently in the model if the food set is sufficiently diverse. This model was initially formulated in terms of the reaction graph only, but was later extended to include rates and concentrations (Farmer et al. 1986; Bagley and Farmer, 1991). Although Kauffman (1986) refers to the polymers as proteins, the model is defined in an abstract way and could just as well apply to autocatalytic sets of RNAs. However, template-directed synthesis is not considered, and the reactions apply to specific sequences rather than to any sequence (as with a universal polymerase ribozyme). Thus, these theories represent a metabolism-first view not a replication-first view, whatever the nature of the chemical reactants is thought to be.

Another example of an autocatalytic set model is the graded autocatalysis replication domain (GARD) model of Segré et al. (1998). The food set consists of a large number of possible monomers. Dimers can form between any two types of monomers. Some of the dimerization reactions are catalyzed by some of the dimers. Hence, an autocatalytic set of dimers may emerge.

1.4 The Lipid World and Compositional Inheritance

The lipid world model (Segré et al. 2000; 2001a; 2001b) was originally developed as a simplification of the GARD model. In the lipid world model there is a diverse set of molecules available in the environment. These molecules do not react chemically with one another, but they can form non-covalent assemblies, such as micelles and vesicles, due to the physical interactions between them. New molecules can be added to assemblies and existing molecules can be removed. The rate of addition and removal are dependent on the other molecules in the assembly. The assemblies contain subsets of molecules that together promote the addition of more molecules of the same types – in this sense they are an autocatalytic set. Random splitting of the assemblies occurs when they reach a specified maximum size. Thus, the model has growth and division of entities with a boundary system but no metabolism or genetic system.

The most important aspect of the lipid world model is that it demonstrates compositional inheritance (Segré et al. 2000; 2001a). Even though the assemblies do not possess informational polymers, they do possess information in the form of the non-random composition of the molecules of which they are comprised. If this compositional information is stable over time and is passed on to the two descendant assemblies when splitting occurs, then the system possesses compositional inheritance. The lipid world model highlights this point by removing all the complexities of the chemical reactions. We note that the earlier model of Dyson (1985) considers a molecular assembly that can exchange molecules with the external environment. This system maintains a non-random molecular composition, but growth and division are excluded, so in our view, there is no

inheritance in Dyson's model. The autocatalytic copolymer models (Kauffman, 1986; Farmer et al. 1986) and the GARD model (Segré et al. 1998) also do not directly demonstrate compositional inheritance because they consider only one reaction network rather than a population. However, if metabolism-first theories for the origin of life are correct, then the metabolic reactions have to become associated with compartmentalized individuals that grow and divide, giving rise to populations of protocells containing autocatalytic reactions sets but no informational polymers. Such a population would also have to have compositional inheritance so that the same autocatalytic metabolism would be passed on. Thus, we think that the idea of compositional inheritance is an important concept that goes beyond the original definition of the lipid world model.

1.5 Aims of this Thesis

This thesis presents two theoretical studies of models related to the origin of life. In Chapter 2, we investigate the idea of compositional inheritance in the lipid world. We consider models for the growth and division of populations of molecular assemblies in which the assumptions of the lipid world model are changed in several ways. We make a distinction between catalysis and self assembly and show that this makes a difference in the way the rates are defined for the addition and removal of molecules. We also introduce the spatial arrangement of the molecules in the assemblies. This factor influences the rates of addition and removal but it was not previously considered. We show that the phenomenon of compositional inheritance is robust to these changes, and

this strengthens the argument that some form of compositional inheritance was an important ingredient in the origin of life.

In Chapter 3 we investigate the positive feedback between catalyzing efficiency and average polymer length. With the help of simulation and analytic deduction, we tried to understand the effects of different parameters, such as polymerization rate and polymer escape rate on the behaviour of this system. From the result, we can find out whether evolvability is an inherent property of the polymerization system.

These two approaches are not exclusive to each other, but complementary to each other. Copley et al argued that the template directed RNA polymerase was not the starting point for RNA world but an intermediate stage following autocatalytic network of small ribozyme (Copley et al, 2007). Hunding et al advanced the hypotheses that life originates from prebiotic ecology of co-evolving populations of macro-molecular aggregates composed of complementary prebiotic available compounds (Hunding *et al*, 2006). Instead of bundled together in a single cell, those ribozymes can form a community to help the existence of each other. Szabo et al. (2002) have studied a model of a population of sequences that cooperate with one another to make duplicate copies of the neighbouring sequences. Hence even in the RNA world approach, different RNA molecules carrying out all kinds of necessary functions effectively form an auto-catalytic network. The self-replication of a universal polymerase ribozyme is not enough for the reproduction of the whole system. Proportional reproduction and segregation of essential ribozymes, such as those that perform the functions of energy capture, nucleotide formation, monomer and polymer activation and stabilization, and membrane molecule

formation, are all necessary. To carry out all these functions and act as templates of themselves at the same time, these ribozymes can't be linked together as a single genome. Hence, the information of the system can only be passed on in the form of compositional inheritance, which is a major issue addressed by the metabolism first approach. Only when a translation mechanism is fully established, functions carried out by protein are separated from information recorded by RNA or DNA. With knowledge of RNA polymerization system, we can find out the pathway from simple organic molecules to complex polymers. Studying the properties of composition inheritance will help us understand the behaviour of pre-genome polymer systems. With these two pieces of work, we can appreciate the bigger picture of origin of life evolving from simple to complex, from monomers to a steady reaction system, from molecules constrained by physical and chemical limits to an evolvable system which can adapt to and thrive in all kinds of environments.

Chapter 2

Compositional Inheritance: Comparison of Self-Assembly and Catalysis

2.1 Catalysis versus Self-Assembly

For scientific research, the first and the most important thing is definition. In the studies mentioned in the introduction chapter, the word 'catalysis' is used in several different ways. In the usual sense of the word, a catalyst is a molecule that speeds up a chemical reaction without taking part in the reaction and without being used up in the process. The molecules in the autocatalytic copolymer models and the GARD model (Segre *et al*, 1998) are catalysts in this sense. In the model of Bagley and Farmer (1991), all polymers of a given length are equivalent thermodynamically and they would all have the same concentration if there were no catalysis or if the system were allowed to proceed to equilibrium. However, when an autocatalytic set arises, the formation of the molecules in the set is catalyzed, and the concentrations of these sequences reach a much higher value than those of the sequences not in the set. This is called 'catalytic focusing'. The concentrations remain out of equilibrium because of continual input and exit of molecules

from the system. The choice of polymers that are included in the autocatalytic set is determined by the catalytic properties of the molecules, not thermodynamic properties.

There are also cases where lipids can catalyze chemical reactions. Bachmann *et al.* (1992) studied an autocatalytic system in which micelles composed of sodium caprylate can catalyze the hydrolysis of ethyl caprylate to form more sodium caprylate, which forms more micelles. Fellerman and Solé (2007) also carried out a simulation of lipid aggregation coupled to catalyzed lipid formation. Walde (2006) gives many examples of chemical reactions that are catalyzed by the presence of lipid micelles and vesicles. However, in the context of the lipid world, the word catalysis is often used in a different way. Szathmary *et al.* (2005) state that 'it is important to point out that membrane growth is an autocatalytic process'. This is correct in the sense that the presence of the membrane promotes the addition of further molecules to the membrane, but in this case it is thermodynamics that drives the addition of the new molecules, not catalysis. The reason lipids form micelles and membranes is because of the interactions between them – the hydrophobic tails have a lower energy of interaction with one another than with water, while the hydrophilic head groups have a lower energy of interaction with the water. Moving a single molecule of lipid from solution to the membrane lowers the free energy of the system. We feel that 'self-assembly' is a better word for what is happening when lipids form micelles or membranes, and that 'catalysis' should be avoided in this context.

The term catalysis is also used in cases where there is a barrier between two states, and the catalyst acts to lower this barrier. An example like this in modern cells is a membrane protein that forms a channel though which a charged molecule can cross a

membrane. The membrane would otherwise be almost impermeable to the charged molecule. The membrane protein clearly speeds up the configurational change without being used up in the process, and it may be legitimate to call it a catalyst. However, molecules as complex as membrane proteins were not around at the time envisaged in the lipid world model. In the lipid world models of Segré *et al.* (2000; 2001a,b), catalysis is used to refer to speeding up the addition or removal of a molecule. It seems likely that a new lipid would be added rapidly because it is attracted to the other molecules in the assembly, rather than because there is a barrier for addition that is somehow lowered by the other molecules. Therefore the 'barrier-crossing' usage of catalysis also does not seem very appropriate for lipid assemblies.

This distinction is not just a matter of words. It becomes important when we consider the rates of addition and removal of molecules of different types. If a molecule of a certain type has a favourable energetic interaction with the existing molecules in the assembly then its rate of addition should be rapid. Once it is added to the assembly, its rate of removal should be slow because there will be an increase in energy going in the reverse direction. Conversely, if a molecule of another type has an unfavourable energetic interaction with the existing molecules then its rate of addition will be slow and its rate of removal will be fast, if it is added. However, this is *not* what happens in the kinetic equations used in previous lipid world models (equation 4 of Segré *et al.* 2000, and equation 10 of Segré *et al.* 2001a). According to these equations, if the rate of addition of one type of molecule is fast, then the removal is also fast, or alternatively, if the addition rate of another type of molecule is slow, the removal rate is slow. These equations

represent catalysis in the sense that both forward and backward reactions are speeded up equally. As a result, the composition of the assembly is determined by catalytic focusing, as in the copolymer autocatalytic set models. This would make sense if we were describing something like the membrane protein above, because the protein would speed up the passage of the charged molecule in both directions, but it seems less reasonable to us in the case of formation of lipid micelles and membranes. We expect the differences in the thermodynamic properties of the molecules to be more important in determining the constituents of an assembly than the differences in their catalytic properties. Therefore, in this paper we define a model of self-assembly in which the rates of additional and removal of molecules are controlled by their thermodynamic properties.

Another detail of the equations of Segré *et al.* is that the rate of addition of a molecule depends on the concentration of all the other molecules in the assembly. This means that the new molecule mixes freely with all the other molecules and is able to interact with all of them. It is more reasonable to suppose that a molecule will only interact with its spatial neighbours. The spatial arrangement of molecules is likely to be important because the differences in thermodynamic interactions between the molecules will lead to attraction or repulsion of molecules of different types. We will therefore include the effects of spatial arrangement and segregation of molecules in the models we discuss here.

2.2 Model Definitions

We suppose that K different types of molecules are present in the external environment from which assemblies may form. The total concentration of molecules is C, and the concentration of each type is C/K. We consider a population of N individual assemblies. Assemblies may grow or shrink by exchange of molecules with the environment. When the number of molecules in an assembly reaches a maximum size M, the assembly splits into two offspring of size $M/2$. At this point, another randomly-chosen individual is removed from the population so that N stays fixed. The molecules in each assembly are arranged in a ring, *i.e.* a one-dimensional array with periodic boundaries. Each molecule interacts only with its two neighbours in the ring. This is the simplest structure in which the spatial arrangement of the molecules is relevant. It is intended as a contrast to the model of Segré *et al.* (2000) in which all molecules in an array interact

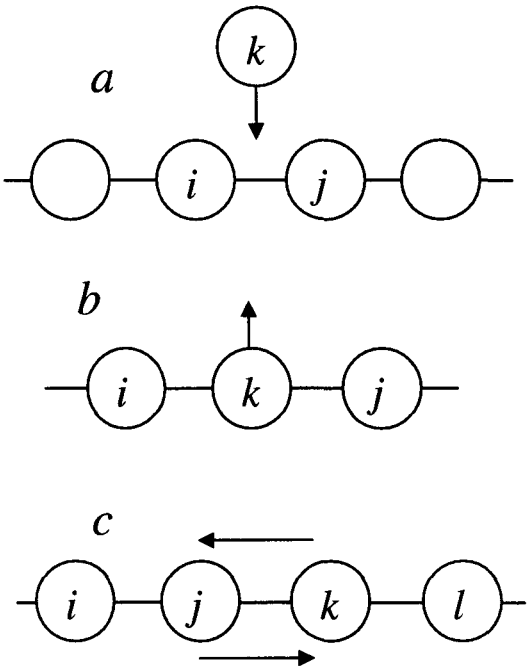

Figure 2.1: (a) Addition of a type k molecule between molecules of types i and j. (b) Removal of a type k molecule from between molecules of types i and j. (c) Diffusive exchange of position of molecules of types j and k between molecules of types i and l.

with one another simultaneously. When a ring splits, one break point is chosen at random and the other break point is chosen to be on the opposite side of the ring. The two half-size rings are then reconnected by establishing periodic boundaries within each one.

Let *i, j, k* and *l* label types of molecules chosen from the *K* possible types. Let $r_{add}(k \mid ij)$ be the rate of addition of a type *k* molecule between molecules of types *i* and *j* (Figure 2.1a), and let $r_{rem}(k \mid ij)$ be the rate of removal of a type *k* molecule from between molecules of types *i* and *j* (Figure 2.1b). We also allow diffusion of molecules within an assembly by exchange of neighbouring molecules. Let $r_{dif}(jk \mid il)$ be the rate of exchange of molecules of types *j* and *k* between molecules of types *i* and *l* (Figure 2.1c). We now define two models: a self-assembly model, in which the rates depend on interaction energies, and a catalytic model, in which the rates depend on catalytic properties.

Self-assembly model: In this case there is a matrix ε_{ij} of energies of interaction between pairs of molecules of different types. The energy of an assembly is the sum of the interaction energies of all pairs of neighbours in the ring. The change in energy when the molecule of type *k* is added in Figure 2.1a is $\Delta E_{add} = \varepsilon_{ik} + \varepsilon_{kj} - \varepsilon_{ij}$. The change in energy when the molecule of type *k* is removed in Figure 2.1b is $\Delta E_{rem} = -\Delta E_{add}$. The change in energy when molecules of types *j* and *k* exchange positions in Figure 2.1c is $\Delta E_{dif} = \varepsilon_{ik} + \varepsilon_{jl} - \varepsilon_{ij} - \varepsilon_{kl}$. To satisfy detailed balance, we require that the ratio of addition and removal rates be

$$\frac{r_{add}(k \mid ij)}{r_{rem}(k \mid ij)} = \frac{C}{K}\exp(-\Delta E_{add} / k_B T) \tag{2.1}$$

where k_B is Boltzmann's constant and T is the absolute temperature. Although this ratio is defined by thermodynamics, there is still flexibility in how the absolute values of the rates are defined. It is standard in Monte Carlo simulations of physical systems to set 'downhill' reactions to rate 1, and the corresponding uphill reactions to be slower by a factor of $\exp(-\Delta E / k_B T)$. However, if we do this, all reactions that are energetically favourable will occur at the same rate. Instead, we will define the rates in the following way:

$$r_{add}(k \mid ij) = \frac{C}{K}\exp(-\Delta E_{add} / 2k_B T),$$
$$r_{rem}(k \mid ij) = \exp(+\Delta E_{add} / 2k_B T) = \exp(-\Delta E_{rem} / 2k_B T). \quad (2.2)$$

With these choices, the reactions that are most energetically favourable will occur fastest. The more strongly attracted a molecule is to the assembly, the faster it will add to the assembly and the slower it will be removed. Often reaction kinetics is described in terms of transition states - in this case, a half-inserted molecule. The rates above assume either that there is no barrier associated with the half-inserted molecule, or that the barrier is systematically lower for molecules that have a lower free energy when fully inserted.

The ratio of the rate of exchange of j and k to the reverse exchange must also satisfy detailed balance:

$$\frac{r_{dif}(jk \mid il)}{r_{dif}(kj \mid il)} = \exp(-\Delta E_{dif} / k_B T). \quad (2.3)$$

We define these rates as:

$$r_{dif}(jk \mid il) = D\exp(-\Delta E_{dif} / 2k_B T), \quad r_{dif}(kj \mid il) = D\exp(+\Delta E_{dif} / 2k_B T), \quad (2.4)$$

where D is a constant that controls the relative rate of diffusion to addition and removal.

Catalytic Model: In this case, the rates depend on a matrix β_{ij} of catalytic effects instead of a matrix of interaction energies:

$$r_{add}(k \mid ij) = \frac{C}{K}(1 + \beta_{ik} + \beta_{jk}), \qquad r_{rem}(k \mid ij) = (1 + \beta_{ik} + \beta_{jk}). \tag{2.5}$$

This is similar to the model of Segré *et al.* because the rates of addition and removal of molecule k are affected by catalysis in the same way, so the ratio of addition and removal rates is independent of the type of molecule. However, we keep track of spatial position. The molecule is influenced by its two neighbours only, rather than by the average of the β factors of all the molecules in the assembly, as was the case for Segré *et al.* (2000, 2001a). We suppose that the diffusion is not affected by catalysis. Therefore, we set $r_{dif}(jk \mid il) = D$, independent of the type of molecules exchanged.

Implementation: When simulating these models, the processes that occur need to be chosen stochastically with rates given by the above rules. The implementation of the stochastic simulation described here applies for either of the two models above, although the rates are defined in different ways. By 'site', we refer to the position of one molecule in an assembly. The number of sites in an assembly is the number of molecules that it currently contains. At each Monte Carlo step, one site is chosen at random from the set of all the sites in all the assemblies in the population. Let R_{site} be the sum of the rates of all the processes that could occur at a site. This can be written as

$$R_{site} = r_{rem-site} + \sum_{k} r_{add-site}(k) + r_{dif-site}, \tag{2.6}$$

where $r_{rem\text{-}site}$ is the rate of removal of the molecule currently at that site, $r_{add\text{-}site}(k)$ is the rate of addition of a molecule of type k between the molecule at this site and its neighbour to the right, and $r_{dif\text{-}site}$ is the rate of exchange of the molecule at this site with its neighbour to the right. These rates depend on the types of molecules at the site and the neighbouring sites according to the rules given above for either of the two models. Let

R_{max} be the maximum possible value of R_{site}. As there is a finite number K of possible types of molecule, there is a finite number of local configurations, and R_{max} can be determined straighforwardly. Having randomly chosen the site, one process may occur at this site. With probability $r_{rem\text{-}site}/R_{max}$ the molecule is removed; with probability $r_{add\text{-}site}(k)/R_{max}$ a molecule of type k is added; and with probability $r_{dif\text{-}site}/R_{max}$ two neighbouring molecules are exchanged. In the case where $R_{site} < R_{max}$ there is a probability $1\text{-}R_{site}/R_{max}$ that nothing happens at this Monte Carlo step.

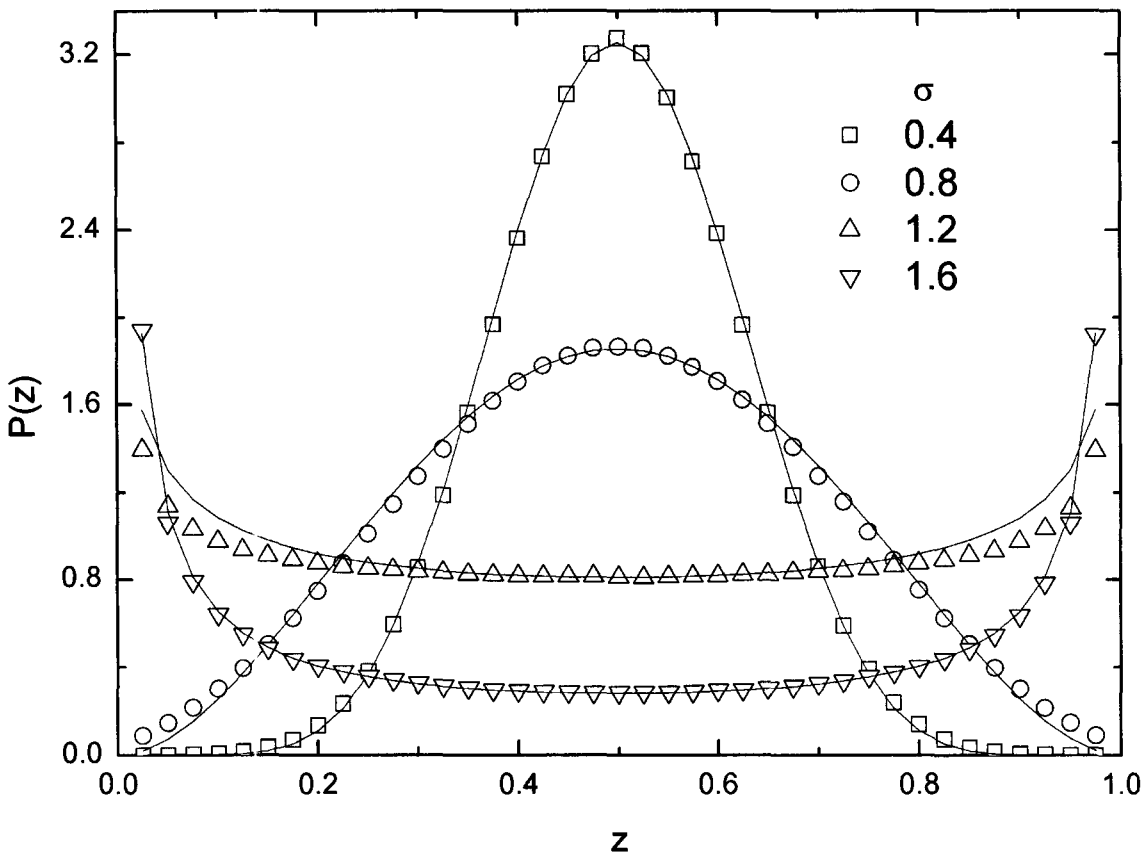

Figure 2.2: Self-assembly model. Distribution $P(z)$ of the fraction of type 1 molecules in an individual at the point where it reaches maximum size. Symbols show simulation results with various values of the energy parameter σ. Curves are fits to the beta distribution to the data.

2.3 Results – Self-Assembly Model

We consider the simplest case with only two kinds of lipids, labelled 1 and 2, and define the interaction energy in terms of an energy parameter a: $\varepsilon_{11} = \varepsilon_{22} = -a$ for molecules of the same type, and $\varepsilon_{12} = \varepsilon_{21} = +a$ for molecules of different types. Note that if some non-zero mean interaction energy were added to all the ε_{ij}, this would not change the model because this factor could be incorporated into C in Eq. 2.1 and 2.2. Therefore we will keep the mean ε_{ij} to be zero. The rates are therefore a function of a single energy ratio $\sigma = a/k_BT$.

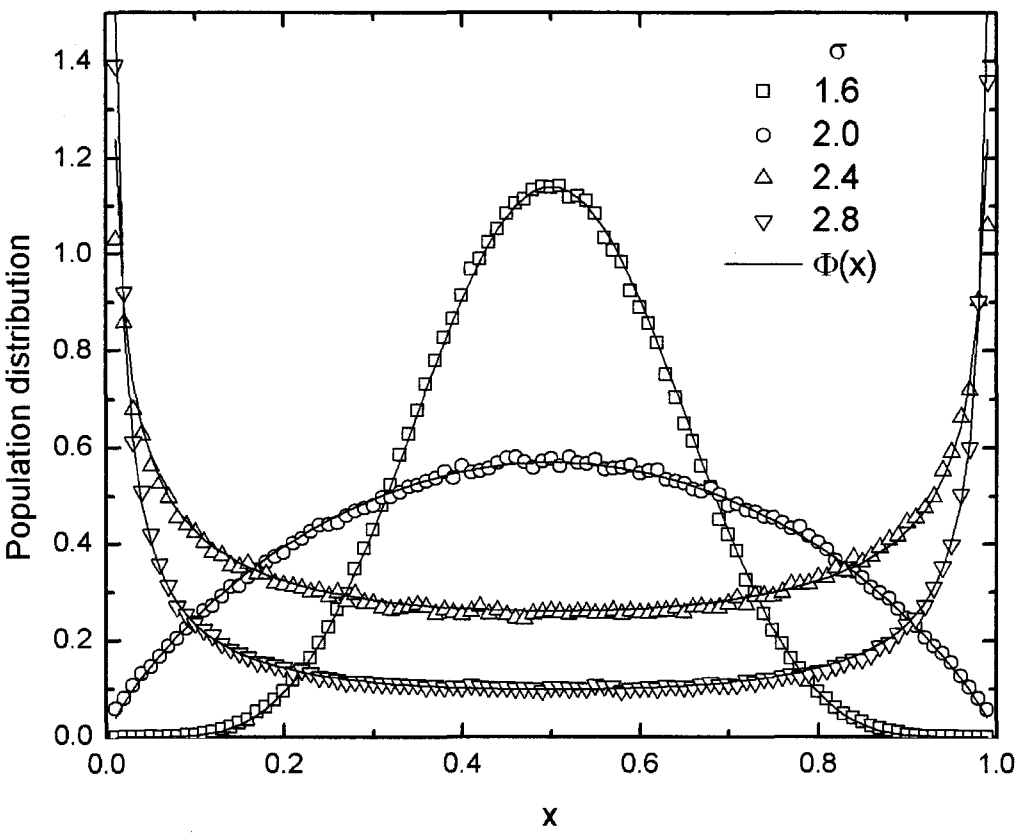

Figure 2.3: Self-assembly model. Distribution $\Phi(x)$ of the fraction of type 1 individuals in the population. Symbols show simulation results with various values of the energy parameter σ. Curves are fits of the beta distribution to the data.

The following simulations were performed with populations of $N = 100$ individual assemblies, using a maximum size of $M = 40$ molecules per assembly. We chose parameters $C = 1.0$ and $D = 1.0$. The simulations began with all individuals containing 20 molecules, each chosen to be 1 or 2 with equal probability. The simulation was run for an initial period to reach a stationary state. After this period, we recorded information on the composition of each assembly at the point of division. $P(z)$ is the probability that an individual has a fraction z of type 1 molecules when it reaches its maximum size M prior to division. Although z is always a multiple of $1/M$, in Figure 2.2, z is treated as a continuous variable, and the curve $P(z)$ is treated as a continuous probability distribution normalized so that there is unit area under the curve. If σ is small, most individuals have a mixed composition (z close to 0.5). If σ is large, most individuals are dominated by either type 1 or type 2 molecules (z close to 0 or 1).

The function $P(z)$ measures variability of molecular composition of individuals. We also want to measure variability at the population level. To do this, we classify individuals as either type 1 or type 2, according to whether they contain a majority of type 1 or type 2 molecules. In the rare case that the two types have equal numbers, the individual is classed as type 1 or type 2 randomly. We then define x as the frequency of type 1 individuals in the population at any given instant in time. The function $\Phi(x)$ is the probability distribution of x. This is obtained by measuring x at regular intervals in the simulation and plotting a histogram of the stored values. The distribution is normalized as though x were a continuous variable, so that there is unit area under the $\Phi(x)$ curve. In Figure 2.3, it can be seen that if σ is small, most populations have a mixed composition (x

close to 0.5). If σ is large, most populations are dominated by either type 1 or type 2 individuals (x close to 0 or 1).

The bell-shaped and U-shaped distributions in Figures 2.2 and 2.3 will be familiar to population geneticists. They are examples of the beta distribution:

$$\Phi(x) = \frac{\Gamma(2\theta)}{\Gamma(\theta)\Gamma(\theta)} x^{\theta-1}(1-x)^{\theta-1}. \qquad (2.7)$$

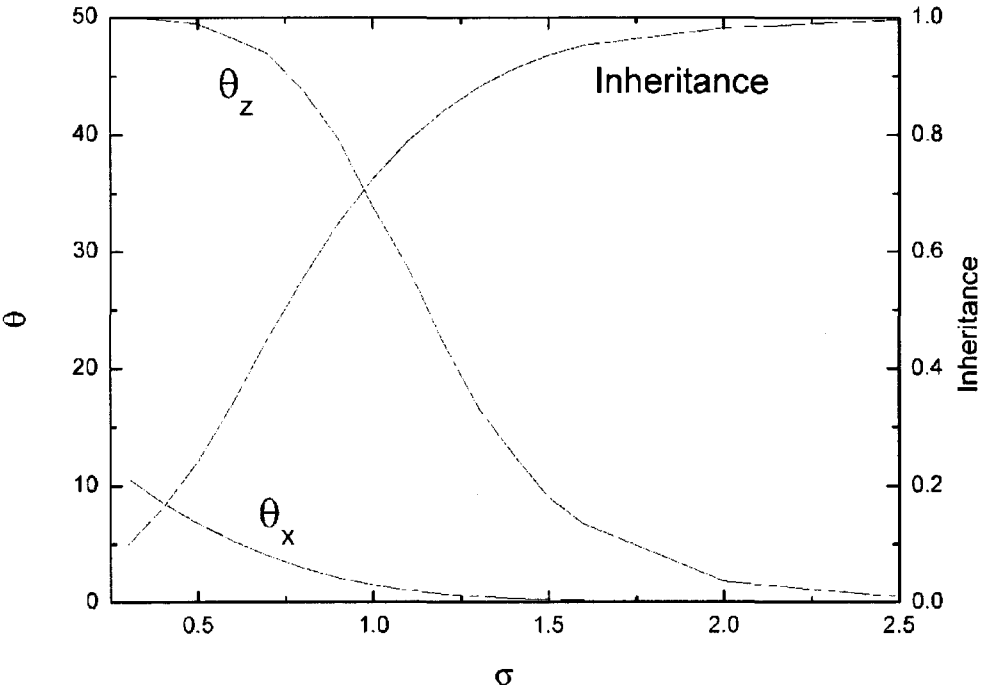

Figure 2.4: Self-assembly model. Left hand scale shows the fitted values of θ for $P(z)$ and $\Phi(x)$ (denoted θ_z and θ_x) as a function of σ. Right hand scale shows the inheritance function I.

The Moran model in population genetics considers the frequency distribution of alternative alleles at a given locus in a population in which genetic drift occurs due to birth and death events (Moran, 1958; Karlin and McGregor, 1962; Ewens, 2004). If there are two alleles with an equal rate of mutation u in both directions between them, then the distribution of frequencies of either allele is given by Eq. 2.7. Allele frequency

distributions are either bell-shaped or U-shaped, depending on the value of θ, which is $2Nu$ in the Moran model. In Figure 2.3, we fitted equation 7 to the $\Phi(x)$ curve from the simulation of the self-assembly model, using θ as a single fitting parameter for each curve. This function fits the data very well. In our case, θ depends on σ rather than u in the Moran model. Large σ corresponds to small u, where the distributions are U-shaped, and lower σ corresponds to higher u, where the distributions are bell-shaped. In Figure 2.2, we used the same beta distribution to fit the P(z) distribution. The function also fits the data quite well. P(z) becomes U-shaped at smaller values of σ than $\Phi(x)$. For example, with σ = 1.6, P(z) is U-shaped but $\Phi(x)$ is still bell-shaped. Thus, for any value of σ, two different θ values are required to fit the two curves. The fitted values of θ are shown as a function of σ in Figure 2.4.

To better understand the analogy between our model and the Moran model, it is necessary to show that there is heredity in our model. We therefore consider the relationship between compositions of parents and offspring. Let z_{parent} be the composition of a parent individual at the point when it reaches size M and is about to divide. Let $z_{offspring}$ be the composition of one of the offspring of this parent at some time later when it has also grown to size M and is about to divide. In the simulations, pairs of parent and offspring compositions were recorded over a long period of time. The contour plots in Figure 2.5 show the probability distribution $p(z_{offspring} \mid z_{parent})$. Horizontal cross sections through the plots are normalized to 1, so that each cross section is a probability distribution for a given z_{parent}.

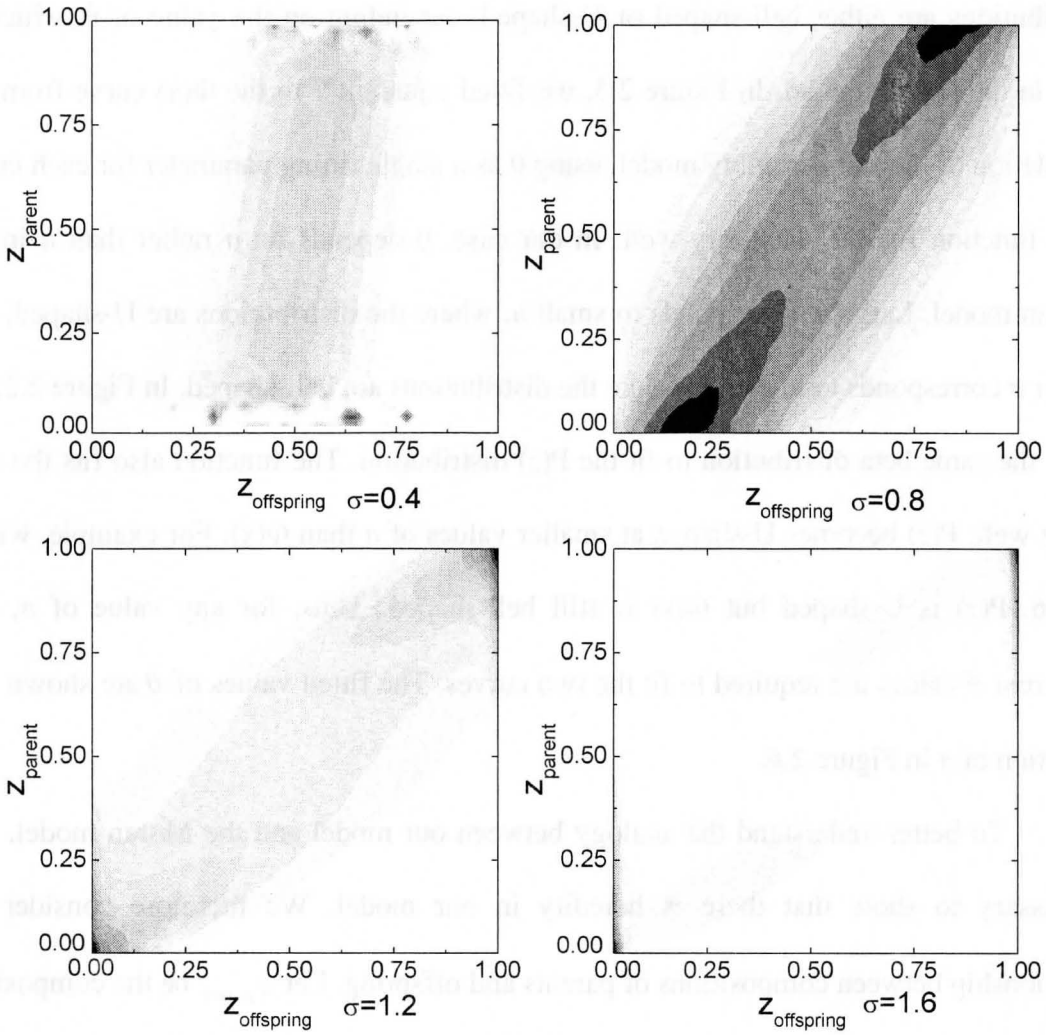

Figure 2.5: Self-assembly model. Probability distributions of the offspring composition $z_{offspring}$ conditional on the composition of their parent z_{parent}.

For σ = 0.4, there is little correlation between parent and offspring. All offspring have composition close to z = 0.5, irrespective of the parent, which means a random mixture of the two types of molecule. In contrast, for σ = 0.8 and 1.2, there is a clear correlation. The mean value of $z_{offspring}$ increases as z_{parent} increases and is fairly close to z_{parent}. There is compositional inheritance in these cases; however, the distribution of offspring compositions is fairly broad, so the heredity is weak. For σ = 1.6, heredity is strong. As $P(z)$ is U-shaped, most parents have compositions close to 0 or 1. The

offspring also usually have composition close to 0 or 1, *i.e.* almost all the weight of the contour plot is in the two corners. The 'spottiness' of the top and bottom of the $\sigma = 0.4$ plot close to $z_{parent} = 0$ and 1 is statistical noise arising from the way the probability is normalized. As $P(z)$ is bell-shaped for this value of σ (see Figure 2.2), there are very few parent individuals with these extreme compositions, so there is very little data contributing to these parts of the plot.

We define the following correlation function I as a quantitative measure of compositional inheritance:

$$I = \frac{\langle z_{offspring} z_{parent} \rangle - \langle z \rangle^2}{\langle z^2 \rangle - \langle z \rangle^2} . \tag{2.8}$$

$I = 1$ if offspring and parents always have identical composition, and $I = 0$ if offspring and parent compositions are uncorrelated. Figure 2.4 shows that I increases with σ, and is close to 1 for σ larger than about 1.5. In this regime, individuals are usually of one extreme composition or other, and offspring are almost always of the same type as their parent.

The analogy between the self-assembly model with two types of molecules and the Moran model with two alleles is quite a strong one. At each time step in the Moran model a single individual multiplies and a single individual dies. In our model the birth and death events are controlled by the growth of the assemblies and do not occur regularly every time step. Nevertheless, when one individual splits, another individual is removed from the population so that the number of individuals remains constant, as in the Moran model. Therefore our model is also a birth and death process. Usually an assembly that is dominated by one type of molecule will grow and divide to produce two offspring

dominated by the same type of molecule. Occasionally, a domain of the other type of molecule may be nucleated and grow, and the assembly may end up being dominated by the other type of molecule. This is the equivalent of a mutation from one type of assembly to another. For this change to occur, the assembly has to pass through high energy configurations with mixed composition. The energy barrier is higher when σ is higher. Hence, the effective mutation rate is lower, and the values of θ needed to fit the $P(z)$ and $\Phi(x)$ distributions are lower.

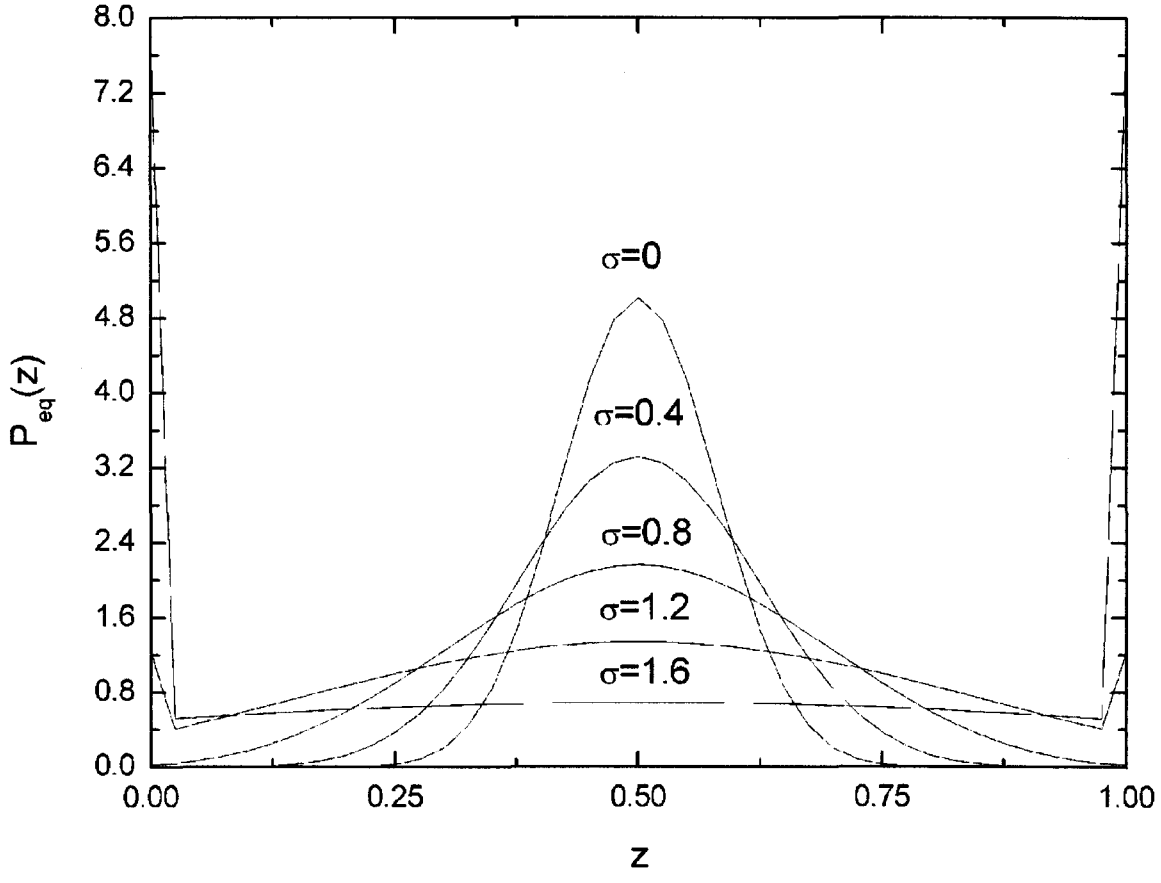

Figure 2.6: Equilibrium composition distribution for a ring of size 40.

With the energies defined as above, molecules of the same type attract one another. Thus within each assembly, the molecules will not be randomly ordered. Instead, there will be alternating domains of molecules of the two types. The larger σ, the larger the

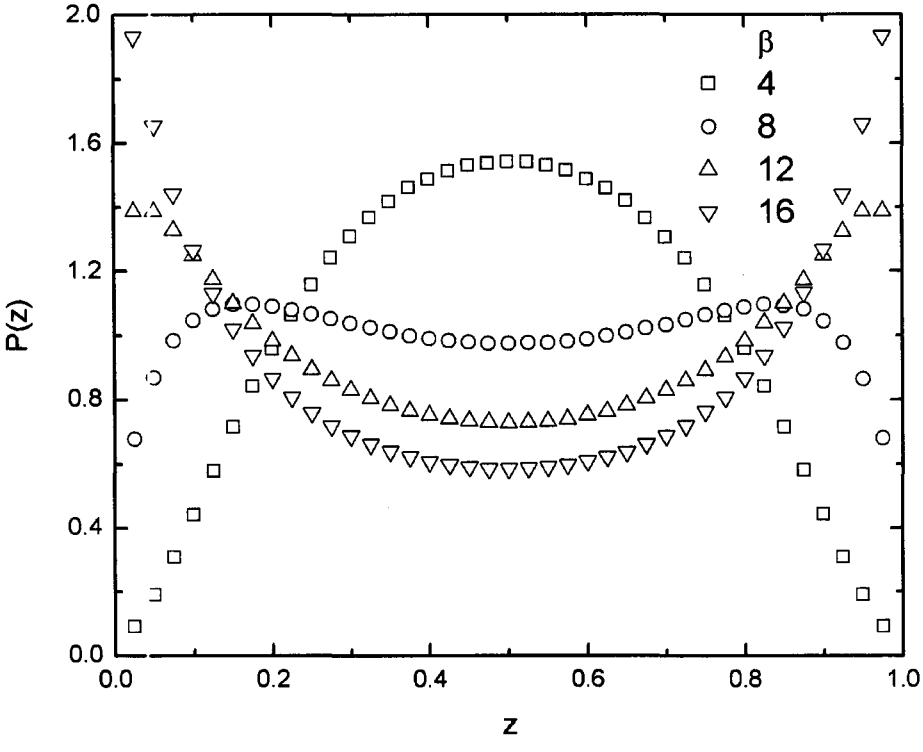

Figure 2.7: Catalytic model. Distribution $P(z)$ of the fraction of type 1 molecules in an individual at the point where it reaches maximum size. Symbols show simulation results with various values of the catalysis parameter β.

typical size of these domains will become. For large enough σ, the typical domain size will exceed the finite size of the assembly itself. Thus, the whole assembly will become a single domain of one type of molecule. The energy rules in this model correspond to the one dimensional Ising model or binary alloy model (Yeomans, 1992). In Figure 2.6, we considered a 1d Ising model on a ring of 40 sites with the same energy rules as used to define the rates. We calculated the partition function exactly numerically, and determined

the probability, $P_{eq}(z)$, that there is a fraction z of molecules of type 1 in the equilibrium ensemble of states. If $\sigma = 0$, the distribution binomial (determined only by entropy). As σ increases, the peak broadens, and for sufficiently large σ, the distribution is dominated by the two extremes. Although qualitatively similar to Fig. 2.2, the shapes are not the same and the curve is not well fitted by a beta distribution. One way of achieving this equilibrium distribution in a dynamical simulation would be to consider a ring of fixed size and use moves that exchange one molecule in the ring for a random molecule from the exterior. This equilibrium system would not be a good model of the system of growth and division that we are interested in here. Assemblies in our system do not have a fixed size. There is either steady growth or steady shrinkage, depending on the external concentration of molecules, C. It would be possible to find a specific value of C where the average growth rate is zero, but there would still be large size fluctuations among assemblies. Our system is maintained out of equilibrium by the continual process of addition of new molecules and division of the assemblies. Growth and division are essential parts of this model, and it is not equivalent to the equilibrium model.

2.4 Results - Catalytic Model

We will now compare the self assembly model with the catalytic model in which there are also just two types of molecule. We will define a single catalytic rate parameter β and set the catalysis factors $\beta_{11} = \beta_{22} = \beta$ for molecules of the same type, but $\beta_{12} = \beta_{21} = 0$ for molecules of different types. In the self-assembly model, it is obvious that molecules will separate into domains of the same type. In the catalytic model, this is less

obvious, because although molecules of each type catalyze the addition of further molecules of their own type, they also catalyze their removal. Nevertheless, compositional inheritance does occur in this model and the results are qualitatively similar to the self-assembly model.

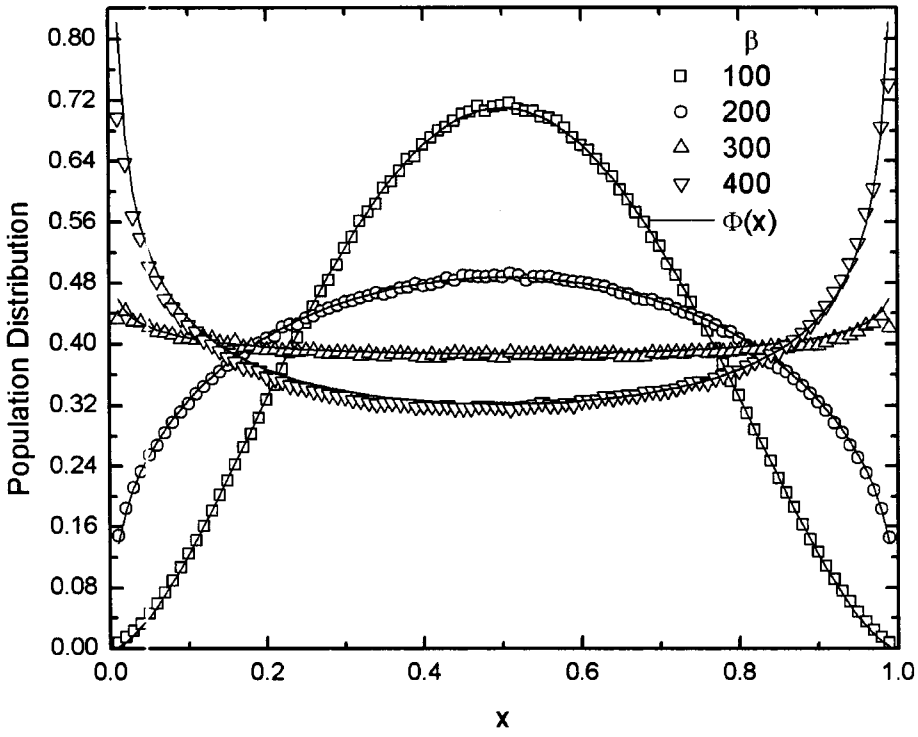

Figure 2.8: Distribution $\Phi(x)$ of the fraction of type 1 individuals in the population. Symbols show simulation results with various values of the catlysis parameter β. Curves are fits of the beta distribution to the data.

We chose parameters $N = 100$, $M = 40$, $C = 5.0$ and $D = 1.0$. Figures 2.7 and 2.8 show $P(z)$ and $\Phi(x)$ in the catalytic model, defined in the same way as for Figures 2.2 and 2.3. Larger values of β correspond to more U-shaped probability distributions and stronger heredity. $P(z)$ becomes U-shaped around $\beta = 8$, but very high values of β around 300 are required before $\Phi(x)$ becomes U-shaped. High values of β are also required

before high heredity values (I close to 1) are obtained. Figure 2.9 shows I, and the two values of θ as a function of β. The plots of $p(z_{offspring} \mid z_{parent})$ for this model are qualitatively similar to those for the self-assembly model and are shown in Figure 2.10. The $\Phi(x)$ measurements are well fitted by the beta distribution, as is shown on Figure 2.8. The shapes of the $P(z)$ distributions are not well described by the beta distributions; therefore we have not added these fitting curves to Figure 2.7.

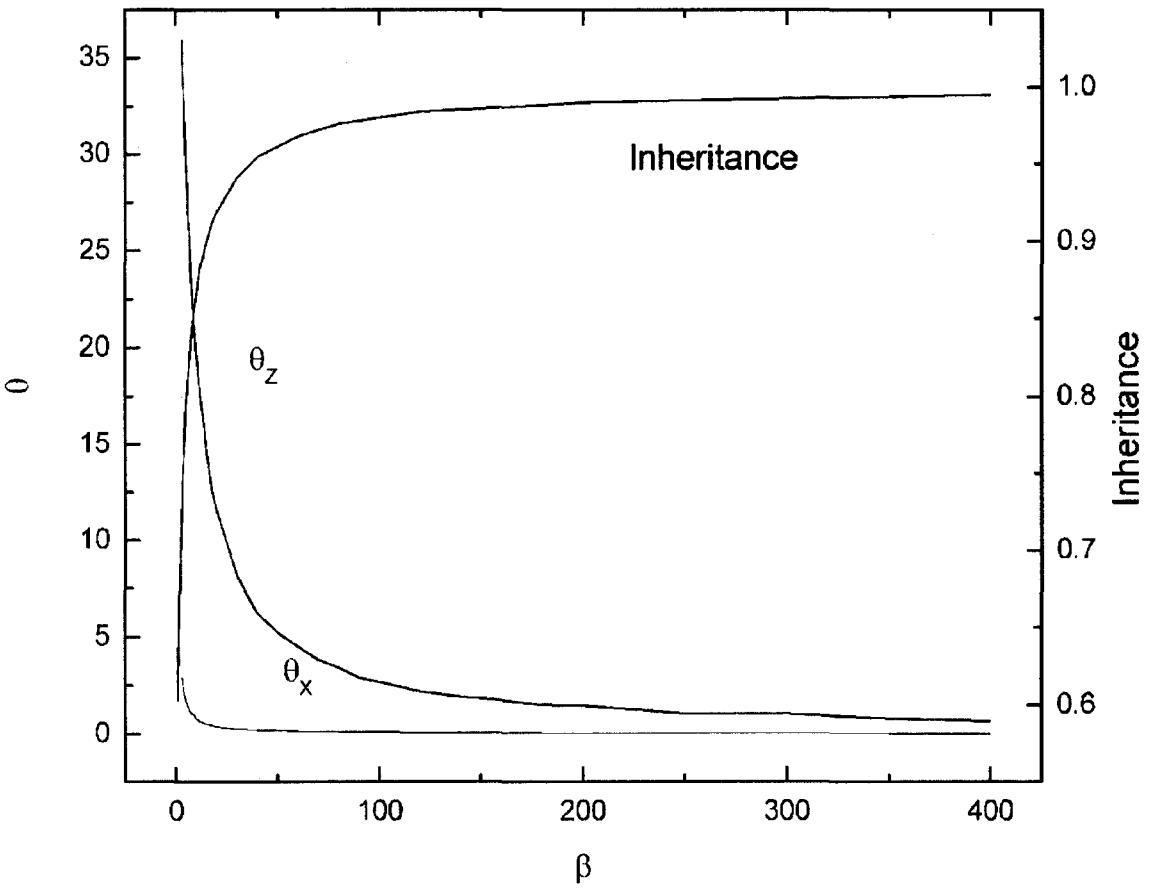

Figure 2.9: Left hand scale shows the fitted values of θ for $P(z)$ and $\Phi(x)$ (denoted θ_z and θ_x) as a function of β. Right hand scale shows the inheritance function I.

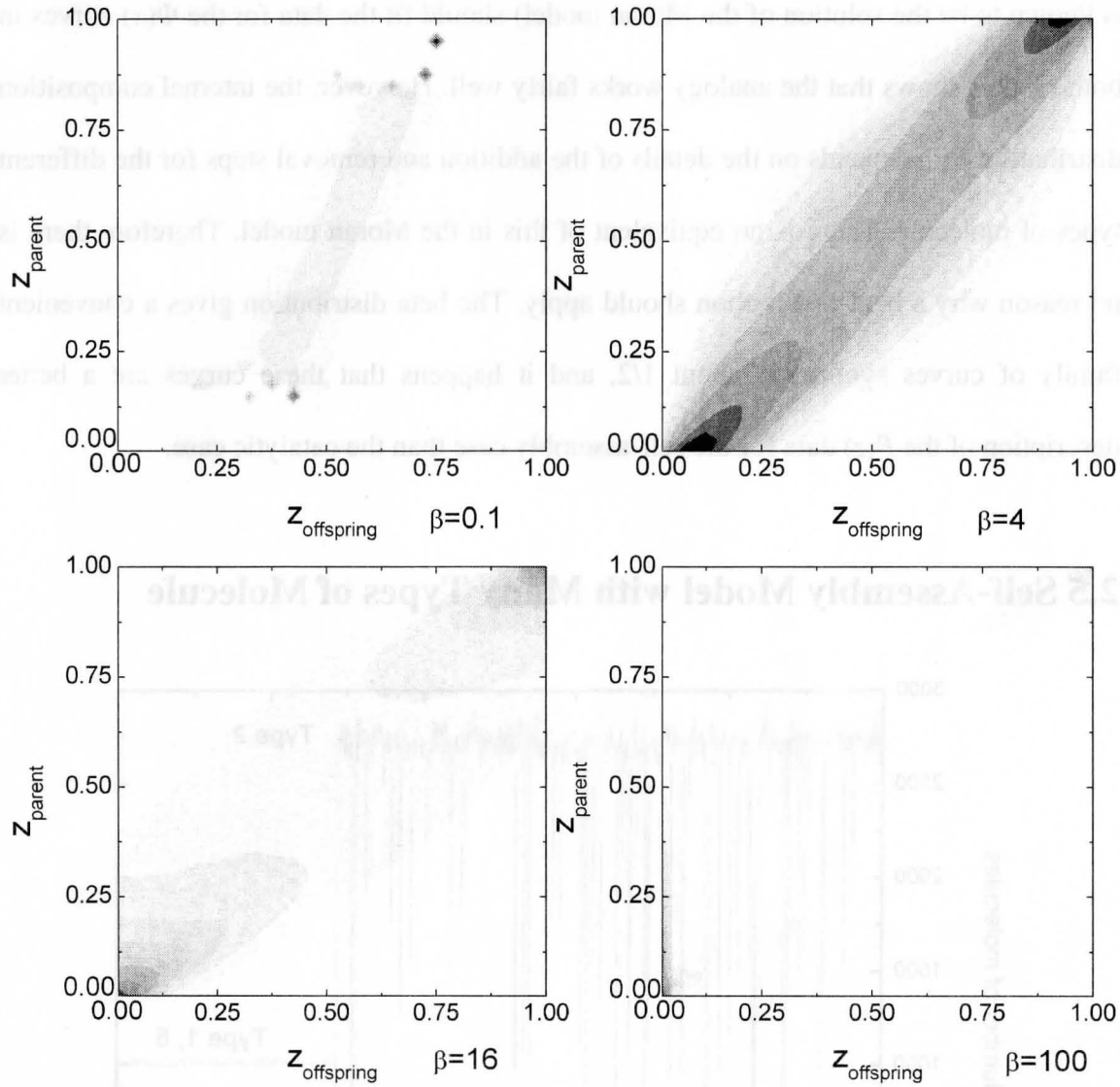

Figure 2.10: Probability distributions of the offspring composition $z_{offspring}$ conditional on the composition of their parent z_{parent}.

For both models, the analogy with the Moran model at the population level is quite strong, because our model is also a birth and death process and we are considering two types of assemblies that are analogous to the two alleles in the Moran model. The analogy is nevertheless not exact, because by counting assemblies as one of just two types, we lose information on the internal composition. The fact that the beta distribution (which

is known to be the solution of the Moran model) should fit the data for the $\Phi(x)$ curves in both models shows that the analogy works fairly well. However, the internal composition distribution $P(z)$ depends on the details of the addition and removal steps for the different types of molecule. There is no equivalent of this in the Moran model. Therefore there is no reason why a beta distribution should apply. The beta distribution gives a convenient family of curves symmetric about 1/2, and it happens that these curves are a better description of the $P(z)$ data for the self-assembly case than the catalytic case.

2.5 Self-Assembly Model with Many Types of Molecule

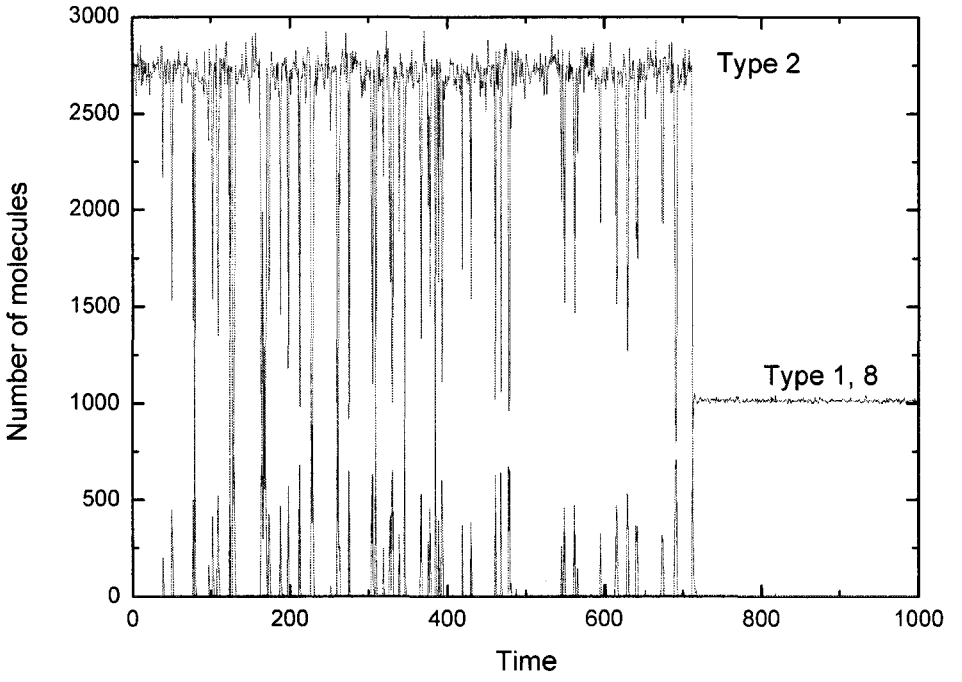

Figure 2.11: Self-assembly model with 10 types of molecules and interaction energies as in Table 2.1. Standard deviation of energies is such that $\sigma = 8$. The number of molecules of types 1, 2 and 8 are shown as a function of time. Other parameter values are $N = 100$, $M = 40$, $C = 1.0$ and $D = 1.0$. At the beginning of the simulation, each assembly has 20 type 2 molecules.

The results presented above have dealt with the simplest case of only two types of molecule because this is sufficient to demonstrate the principle and because the genetic analogy is easiest to see. However, the stable compositions are uniform in this case. It is already known that the lipid world models of Segré *et al.* (2000, 2001a,b) stable compositions arise that contain mixtures of molecules. Therefore, in this section, we briefly investigate the self-assembly model in the case where the number of types of molecule, K, is greater than two, and show that stable compositions with more than one type of molecule can arise. There are $K(K+1)/2$ possible nearest neighbour interactions. We assume that the energy ε_{ij} of each interaction is chosen randomly from a Gaussian distribution with mean value of 0 and a standard deviation such that $< \varepsilon_{ij}^2 >^{1/2} / k_B T = \sigma$.

Table 2.1 shows the values of $\varepsilon_{ij}/k_B T$ in an example of one such random matrix for ten types of molecules with $\sigma = 8$. The most negative element on the diagonal is ε_{22} and the most negative off-diagonal element is ε_{18}. The two most stable molecular configurations are the uniform configuration 222222 and the alternating configuration 181818. Figure 2.11 shows the number of molecules of each type in a simulation that begins with all individuals composed only of 2's. Since the population size is $N = 100$, and the maximum assembly size is $M = 40$, the maximum number of molecules is 4000. The actual number is less than this because there is a distribution of sizes of assemblies that are smaller than M. The number of 2's remains high in the population for a long time because most individuals consist of strings of 2's. In the early part of the simulation, 1's and 8's show up as sharp peaks. This is due to the presence of a few individuals with mixed domains such as 18181822222. Later in the simulation, individuals exclusively of

18181818 arise and out-compete the 222222 individuals. The number of 2's then falls to a very low level that is not visible on this scale. The numbers of molecules of types other and 1, 2, and 8 are also too low to be visible on this scale. In both Figures 2.11 and 2.12, the numbers of types 1 and 8 are too close to be distinguishable from one another, which indicates that these molecules almost always occur in blocks of 181818.

	1	2	3	4	5	6	7	8	9	10
1	11.34	3.39	-8.39	-6.64	14.70	-5.11	12.76	-25.65	1.26	-2.28
2	3.39	-12.37	-5.34	12.13	23.06	0.40	2.15	-0.09	8.22	-1.83
3	-8.39	-5.34	19.76	-7.24	6.46	-2.02	10.56	1.91	-11.42	-5.95
4	-6.64	12.13	-7.24	3.63	9.42	-8.79	7.37	-8.76	-2.73	-11.19
5	14.70	23.06	6.46	9.42	-1.81	10.62	5.05	-3.34	-5.16	-5.47
6	-5.11	0.40	-2.02	-8.79	10.62	-2.70	-8.49	10.43	8.04	4.80
7	12.76	2.15	10.56	7.37	5.05	-8.49	4.92	-6.57	2.90	-3.74
8	-25.65	-0.09	1.91	-8.76	-3.34	10.43	-6.57	10.95	17.17	1.78
9	1.26	8.22	-11.42	-2.73	-5.16	8.04	2.90	17.17	-6.14	5.96
10	-2.28	-1.83	-5.95	-11.19	-5.47	4.80	-3.74	1.78	5.96	6.20

Table 2.1: Random matrix of interaction energies with standard deviation $\sigma = 8$.

Figure 2.12 shows a simulation with $\sigma = 4$, such that the values of ε_{ij}/k_BT are half those shown in Table 1. In this case neither of the stable configurations dominates the whole population. Instead, there is a mixture of individuals of each of the two stable configurations and individuals with mixed domains. The frequencies of the other types of molecule are lower than 1, 2, and 8, but are high enough to be visible at this value of σ. Another interesting thing in Figure 2.12 is that the 222222 configuration is more frequent than 181818, even though the latter has the lower energy. This is because the 181818 configuration grows more slowly at this value of σ. The alternating configuration has the disadvantage that both ε_{11} and ε_{88} are positive in this random matrix, so inserting either a

1 or an 8 into the alternating configuration is slow. We have observed that growth of the alternating configuration can be aided by defects such as 1818418181, because both ε_{41} and ε_{48} are negative and 1's and 8's can be easily added next to the defect. Another disadvantage of the alternating configuration is that it can be disrupted by diffusion, *i.e.* 181818 becomes 188118, and removal of the two molecules that were exchanged then becomes favourable. In the case of 222222, diffusion makes no difference. The relative advantages and disadvantages of different configurations depend on σ. We already saw that 181818 out-competes 222222 at σ = 8. The above results confirm that compositional inheritance occurs in the self-assembly model in cases where there are many types of molecule available and that it is possible to have stably inherited compositions that contain more than one type of molecule.

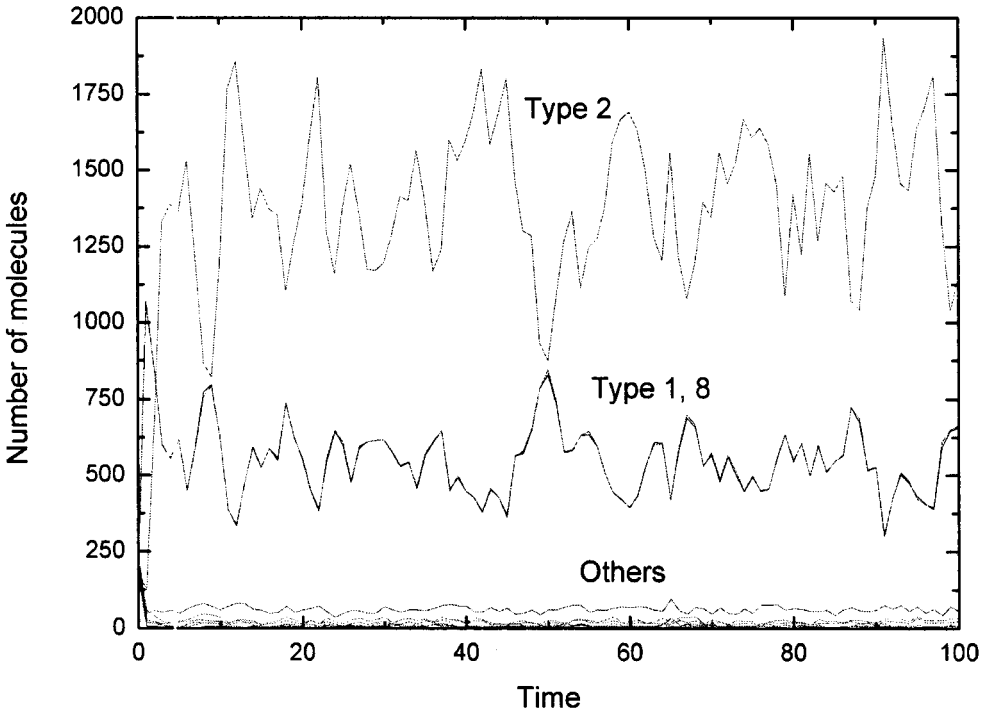

Figure 2.12: As Figure 2.11 except that σ = 4. Low numbers of molecules of types other than 1, 2 and 8 are also visible.

2.6 Discussion and Conclusions

Inheritance means the passing on of information from an individual to its descendants. It is well known that this can be done by copying gene sequences, but the lipid world models demonstrate that compositional information can also be passed on without genes. It is pleasing that there should be such a good analogy between the models studied here and the Moran model, which is a classic model in population genetics. This underlines the fact that compositional inheritance really is a form of inheritance.

Compositional inheritance has previously been discussed mainly in the context of one particular version of the lipid world model (Segré *et al.* 2000, 2001a,b). Our object here has been to investigate to what extent the same phenomenon occurs in models that are defined in significantly different ways. We argued that the self-assembly of lipid micelles and vesicles is driven by the thermodynamics of the interactions between them, rather than by catalysis. Therefore we studied a model for self assembly, in which the molecules differ in the energy of the interactions between them, and compared this to a model for catalysis, in which the molecules differ in their catalytic properties. The result is that both models show compositional inheritance, but for different reasons. In the self-assembly model, non-random compositions of molecules arise because they have mutually attractive interactions, whereas in the catalytic model they arise because of mutually favourable catalysis.

In the preceding section on multiple types of molecules, we tested only the self-assembly model and not the catalytic model. We believe that the latter would also show

compositional inheritance, as has already been demonstrated in the catalytic models of Segré *et al.* However, we did not pursue the catalytic model with multiple types because, if the model is supposed to represent very simple molecules like lipids, the kinetic rules of the self-assembly model make much more sense that those of the catalytic model. It is clear that interaction energies between neighbouring molecules can differ according to what types of molecules are involved. On the other hand it is not clear that simple lipids have the ability to be very specific catalysts. Values of β in the hundreds are required for the catalytic model to work well. One can imagine highly adapted catalysts, such as membrane proteins, greatly speeding up both the addition and removal of molecules from a cell; however, it seems unlikely that a simple lipid could cause one type of neighbouring molecule to slide into an assembly a hundred times faster than an alternative type and also cause it to slide out a hundred times faster, and yet have identical interaction energy with the two types. Thus, although we have shown that compositional inheritance works for both self-assembly and catalytic models, we feel the self-assembly model is more relevant for assemblies of simple molecules.

Previous lipid world models included no spatial structure. In the self-assembly model, we argued that differences in interaction energies between different types of molecules are sufficient to affect the composition of assemblies. If so, then these differences in interaction energies will be sufficient to cause spatial segregation of molecules. Therefore it seems important to us to account for spatial structure in these models in some way. We used a one-dimensional ring structure because this is very simple to simulate. We presume that compositional inheritance would also occur in

models with a two-dimension membrane structure or a three-dimensional globule structure. One dimension is the least favourable case for this kind of model because there is no long-range order. For example, there is no finite temperature phase transition in the one dimensional Ising model, whereas a phase transition does occur in two and three dimensions (Yeomans, 1992). Thus, the fact that compositional inheritance does occur in both of our models argues for the generality of the phenomenon, and suggests that compositional inheritance is a concept that has broad relevance beyond the specific example of the model in which it was introduced. Whilst on the subject of spatial arrangement of catalysts, we note that a different point is illustrated by the model of Bradford and Dill (2007), which shows that catalysts that have substrates or products in common tend to associate spatially to form complexes carrying out more than one reaction.

Even though the models we studied demonstrate physical interactions between molecules are sufficient to cause non-random assemblies and to cause inheritance of compositional information, we are still somewhat dissatisfied with the lipid world scenario. It is difficult to see how such assemblies can evolve towards more complex systems unless we incorporate chemical reactions into the model. Dimerization reactions were in fact included in the original GARD model (Segré *et al.* 1998), but were later removed. Dimers and trimers have been re-added in the latest version (Shenhav *et al.* 2007). Chemical reactions create a much higher degree of diversity than would be present in the environment, and they lead to the possibility of forming an autocatalytic set of reactions that remains in a non-equilibrium state, like the metabolism of a cell. In the

various versions of the GARD model, there are already a large number of monomers and diversity further increases by forming dimers and trimers. In the models for autocatalytic sets of copolymers (Kauffman, 1986; 1993; Farmer *et al.* 1986; Bagley and Farmer 1991), diversity arises because of the exponential number of polymer sequences that can be made from a small number of monomers. This latter case seems more reasonable as a model for either nucleic acids or proteins. Models of copolymer autocatalytic sets have dealt with large deterministic systems and have not so far considered compartments, but it seems reasonable to consider that lipid vesicles may have housed such reaction sets. In this context, we note that Goldstein (2006) has studied another model of populations of assemblies containing complex reaction networks, and finds that compositional inheritance occurs. However, the rates of increase and decrease in molecular concentrations were taken to be linear functions of the concentrations of the other molecules, and it is not clear that these equations are a good description of the rates of reactions in autocatalytic sets. In general, compositional inheritance would be relevant for vesicles containing autocatalytic sets because the correct mix of chemical reactants would have to be passed on when the vesicle divided. However, it would not be reasonable to call this a lipid world. The molecules involved in the reactions would probably not be lipids, and the role of the lipid might simply be to form the membrane that houses the reactions. One single type of lipid could do this job, and there need be no information or heredity within the membrane itself.

Luisi *et al.* (1999) and Walde (2006) have emphasized the many roles that surfactant assemblies may have in the origin of life. The conditions under which shape

changes leading to budding and division of vesicles can occur have been closely investigated theoretically (Seifert *et al.* 1991; Bozic and Svetina, 2004; Macia and Sole, 2007). There has also been a lot of experimental progress towards the construction of systems in which some aspects of living cells are contained within self-assembled lipid vesicles (Pohorille and Deamer 2002; Hancyk and Szostak, 2004; Luisi *et al.* 2006; Solé *et al.* 2007; Monnard *et al.* 2007). These experiments demonstrate that lipid vesicles have the right chemical and physical properties to act as environments for early molecular evolution. However, they stop short of demonstrating inheritance of compositional information in the lipids. In fact, we know that modern cells are crucially dependent on information-carrying polymers. It is clear that polymers such as RNA evolved very early in the history of life. Once present, they could be used as catalysts and as genetic material and the possibility of evolution via RNA replication and mutation was then opened up. It is difficult to conceive of evolution beyond the most rudimentary level without the presence of long polymers. Therefore it still seems to us that the crux of the problem of the origin of life is to show how autocatalytic sets involving specific sequences of information-carrying polymers arose. Self-assembled lipid vesicles appear to us as the most likely place in which the chemistry of biopolymer synthesis got going. The possibility that the lipid components of the vesicles showed compositional inheritance in their own right is an interesting one, but the creation of the information-carrying polymers within a vesicle environment would not necessarily require this.

Chapter 3

A Model of RNA Polymerization inside Primitive Cells

3.1 Introduction

Prebiotic synthesis of RNA from nucleotides has been investigated for decades and progress has been made (Sleeper and Orgel, 1979; Ferris, 1996; Johnston, 2001), as was discussed in Section 1.2. As an unfavourable reaction in aqueous solution, RNA polymerization by nucleotide condensation is made possible by using activated monomers or by carrying out the process in a dry environment. In both cases, RNA chains that are long enough to have catalytic function can be produced. Although the equilibrium concentrations of a general chemical system won't be changed by catalysts, it may be different for a polymerization system which is constituted of a cascade of infinite number of reactions. Even when forward reaction and backward reaction are accelerated at the same rate, the difference between them is amplified at the beginning of polymerization. It results in the formation of more polymer, which may trigger the polymerization reaction extending those newly formed polymers even longer. With the newly added reactions, those already existing polymers may be consumed to form longer polymers. Hence, the equilibrium concentration of this system is shifted toward longer polymers. In the case of

RNA polymerization, an RNA sequence capable of polymerization catalyzing better than prebiotic ones may cause the formation of longer RNA sequences, among which even more efficient polymerase ribozymes may be produced. If this is true, average polymer length will increase spontaneously, and it is possible for ribozymes with many more functions to emerge. With a length of 100, template directed RNA replicating ribozyme is possible and the gate towards RNA world is opened.

3.2 Model Definition

We want to define the equations describing the polymerization of monomer units (*i.e.* single nucleotides) inside a primitive cell. The RNA backbone is formed by phosphodiester bonds that should be equivalent for the different RNA bases. Therefore, in the first instance, we will ignore the specific sequence of monomers and just consider the polymerization of a single generic type of nucleotide monomer denoted A. A polymer of n nucleotides is denoted A_n. The object is to calculate the distribution of polymer lengths and determine the way this depends on the rates of the different reaction steps. We will suppose that the reaction rate constants are fixed, and are parameters of the model. Our long term goal is to consider cases where long polymers, once formed, can act as catalysts that speed up further polymerization. This would introduce a feedback into the model where the rate constants are functions of the distribution of lengths of polymers formed. However, we have not yet considered this case, and in this chapter, we present results only for the case where the rate constants are fixed and independent of the polymer length distribution.

We will now describe the chemical reactions incorporated into the model. We suppose that spontaneous polymerization of monomers is negligible, and that polymerization requires activated monomers (as discussed in section 1.2). These are denoted A^*. The activation reaction requires free energy input. The simplest way to write this is to suppose that it requires consumption of a high energy 'food' molecule, F.

$$F + A \underset{r_0 / k_0}{\overset{r_0}{\Leftrightarrow}} A^* \quad r_0 : activation\ rate \tag{3.1}$$

The rate constant r_0 controls the forward activation reaction. The ratio of the forward and backward reaction is determined by the equilibrium constant $k_0 = \exp(-\Delta G/kT)$. We suppose that the forward reaction is energetically favourable because it is driven by the consumption of F. Thus, $\Delta G < 0$ for the forward reaction in equation 3.1, and $k_o >> 1$. The backward reaction in equation 3.1 is slow.

Equation 3.2 describes the growth of a polymer by addition of one activated monomer.

$$A_n + A^* \underset{r_1 / k_1}{\overset{r_1}{\Leftrightarrow}} A_{n+1} \quad r_1 : polymerization\ rate \tag{3.2}$$

This equation applies for any n, and we assume that the rate constant r_1 is independent of n. Note that A_1 is synonymous with A. The forward reaction in equation 3.2 is energetically favourable because it releases the energy in the activated monomer. The equilibrium constant k_1 is much greater than 1 for this reaction too.

We also suppose that polymers may spontaneously split at any point along their length. This represents, for example, hydrolysis of an RNA chain.

$$A_n \xrightarrow{r_2} A_i + A_{n-i} \quad r_2 : decomposition\ rate \tag{3.3}$$

The reverse reaction, spontaneous ligation of two polymers, is not only energy unfavourable, but also hard to happen. Hence, we treat this reaction as irreversible. In this reaction scheme, polymers may only grow from the end, one monomer at a time, but they may decompose by splitting at any point.

In addition, we suppose that activated monomers can decay to produce a waste product *W*.

$$A^* \xrightarrow{r_3} A + W \quad r_3 : decay\ rate \tag{3.4}$$

We suppose that the reverse reaction rate is negligible because it would be uphill thermodynamically and because *W* is rapidly released into the environment and so remains at low concentration. The net result of the metabolism is to convert *F* to *W*. Some of the free energy released in this process is used for polymerization.

The reactions above are assumed to occur in a particular place that is favourable for the activation and polymerization reactions, e.g. inside a lipid vesicle or bound to a mineral surface, or within pores in rocks (as discussed in section 1.2). It is necessary to describe exchange of molecules between the inside – *i.e.* the organism in which the metabolism occurs – and the outside environment. We assume that food and monomer exist abundantly in the environment with fixed outside concentration F_{out} and A_{out}. Diffusion of *F* and *A* into and out of the organism is controlled by rate constant u_1.

Formation of A^* only occurs inside the organism. The rate constant for escape of A^* is also u_1. Polymers are also formed inside the organism and can escape at a rate u_2. In general, $u_2 \leq u_1$, because diffusion of the larger molecules is slower or because it is more difficult for larger molecules to cross the membrane of the cell. The case of $u_2 = 0$ is also relevant. In that case polymers are trapped inside the system and only monomers can enter and leave.

It is to be expected that increasing the rates of the activation, r_0, and polymerization, r_1, will increase the quantity and length of the polymers formed. Increasing the escape rate for polymers, u_2, or the breakdown rate of polymers, r_2, should reduce the quantity and length of the polymers. We will consider cases where the length distribution is determined principally by escape and cases where it is determined principally by breakdown. We will show that the expected length distribution of the polymers in different in these two cases.

3.3 Simulation Methods

The simplest way to simulate the reaction system above is to represent it by the set of differential equations below. The symbols *A, F, etc.* should be interpreted as the concentrations of the appropriate molecules.

$$\frac{dA}{dt} = u_1(A_{out} - A) - r_0 FA + \frac{r_0}{k_0} A^* - r_1 AA^* + \frac{r_1}{k_1} A_2 + \sum_{i>1} 2r_2 A_i + r_3 A^* \tag{3.5}$$

$$\frac{dF}{dt} = u_1(F_{out} - F) - r_0 FA + \frac{r_0}{k_0} A^* \tag{3.6}$$

$$\frac{dA^*}{dt} = -u_1 A^* + r_0 FA - \frac{r_0}{k_0} A^* - \sum_i r_1 A_i A^* + \sum_{i>1} \frac{r_1}{k_1} A_i - r_3 A^* \tag{3.7}$$

$$\frac{dA_i}{dt} = -u_2 A_i - r_1 A_i A^* + r_1 A_{i-1} A^* - \frac{r_1}{k_1} A_i + \frac{r_1}{k_1} A_{i+1} - r_2 (i-1) A_i + \sum_{j>i} 2 r_2 A_j \tag{3.8}$$

We assumed that, at t=0 monomer and food molecules start to diffuse into the system, which is an empty space contains only necessary catalyst. These equations were solved numerically using the 4th order Runge-Kutta method (Press et al, 1992). Except in one special case considered below, the concentrations converge to stationary values that are independent of the initial concentrations. Equation 3.8 applies for any value of $i \geq 2$; so in principle, there is an infinite set of equations. In practice, however, we want to represent a system of finite volume, so the concentrations cannot fall below some minimum threshold that represents 1 molecule in the volume of the cell. The results below are performed with a threshold concentration of 10^{-10}. Any concentration below this value is set to exactly zero before the next time step of the Runge-Kutta method. As the concentrations of the long polymers decrease with length, the threshold sets a maximum polymer length that needs to be considered, and ensures that the number of equations is finite. The maximum length is a function of the rate parameters, however.

3.4 Results

3.4.1 Results When Length is Limited by Polymer Escape

Figure 3.1 shows the stationary distribution of polymer concentrations in the case where the polymer breakdown rate, r_2, is zero, and the factor limiting growth of the

chains is the escape of polymers from the system (u_2). Parameter values are listed in the caption to Figure 3.1. In this example we have set $u_2 = u_1$, *i.e.* polymers can escape from the system as easily as monomers. Several curves are shown corresponding to different values of the polymerization rate, r_1, with all the other parameters held constant. The curves are straight lines on a log scale, meaning that the concentration decreases exponentially with length. The cutoff at longer lengths is caused by the minimum concentration threshold.

In the following argument we aim to calculate the exponential part of the concentration distribution, ignoring the finite size cutoff for the moment. The equations are considerably simpler when $r_2 = 0$. When system goes to equilibrium, we have from equation (3.2):

$$\frac{dA_i}{dt} = -u_2 A_i - r_1 A_i A^* + r_1 A_{i-1} A^* - \frac{r_1}{k_1} A_i + \frac{r_1}{k_1} A_{i+1} = 0$$

$$\Rightarrow (u_2 + r_1 A^* + \frac{r_1}{k_1}) A_i = r_1 A_{i-1} A^* + \frac{r_1}{k_1} A_{i+1} \tag{3.9}$$

Suppose polymer concentration decreases exponentially with length, *i.e.* $A_n = Ax^{n-1}$, for some x to be determined. Eq 3.9 can be rewritten as

$$\frac{r_1}{k_1} x^2 - (u_2 + r_1 A^* + \frac{r_1}{k_1}) x + r_1 A^* = 0 \tag{3.10}$$

Define total concentration of polymers in this system as

$$P = \sum_n A_n = \sum_n x^{n-1} A_1 = \frac{x A_1}{1-x} \tag{3.11}$$

At equilibrium, concentrations of all molecules converge to steady state value and all the left side terms of Eq. 3.5- 3.8 equal zero. Hence we can rewrite Eq 3.7 as following

$$0 = -(u_1 + \frac{r_0}{k_0} + r_3)A^* + r_0 F A_1 - r_1 A_1 A^* + (\frac{r_1}{k_1} - r_1 A^*)P$$

$$\Rightarrow r_0 F A_1 = (u_1 + \frac{r_0}{k_0} + r_3)A^* + r_1 A_1 A^* + (r_1 A^* - \frac{r_1}{k_1})\frac{x A_1}{1-x} \qquad (3.12)$$

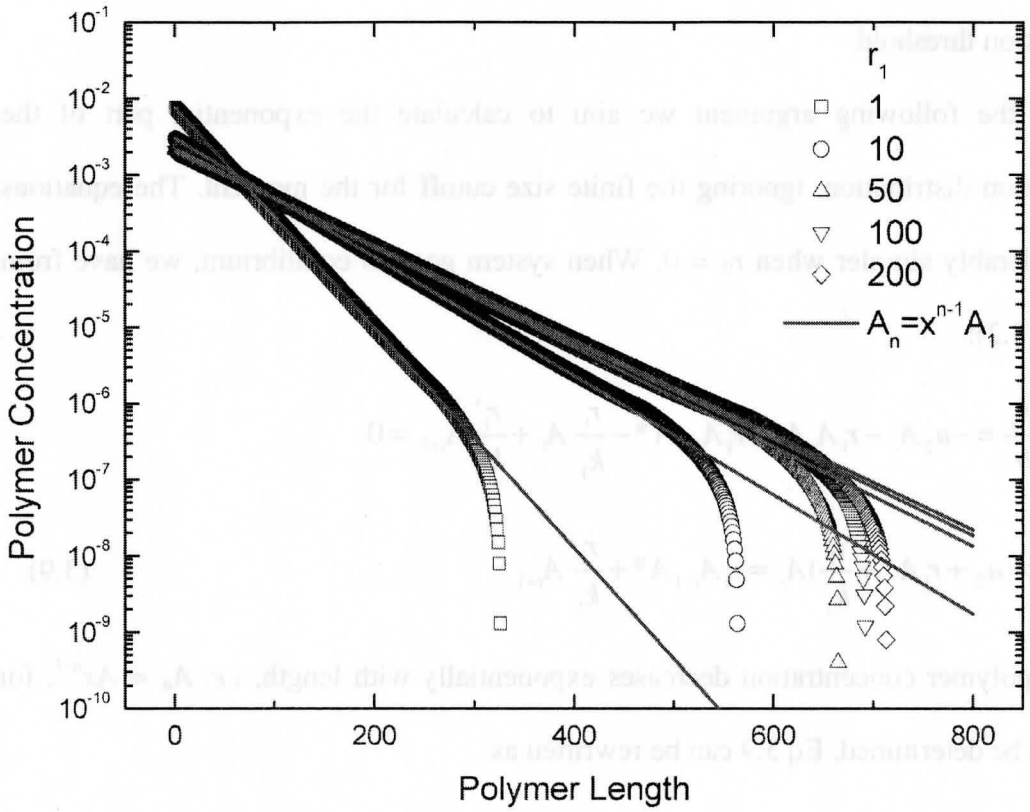

Figure 3.1 Stationary distribution of polymer concentrations as a function of length in the case where the length is limited by the escape rate u_2 and the polymer breakdown rate, r_2 is zero. The following parameters were used k_0=100, k_1=100, r_0=100, r_2=0, r_3=0.001, A_{out}=10, F_{out}=15, u_1=0.1, u_2=0.1

Based on the exponential concentration decay assumption, we substitute $A_2 = xA_1$ into Eq. 3.5:

$$0 = u_1(A_{out} - A) - r_0 FA + \frac{r_0}{k_0} A^* - r_1 AA^* + \frac{r_1}{k_1} xA_1 + r_3 A^* \qquad (3.13)$$

With Eq 3.6, 3.10, 3.12 & 3.13, we can solve A^*, A_1, F and x for different r_1. Hence we can obtain length distribution of polymers. Comparing the solution results with numerical integration result of Eq 3.5-3.8 in Fig. 3.1, we found that they are in consistent with each other.

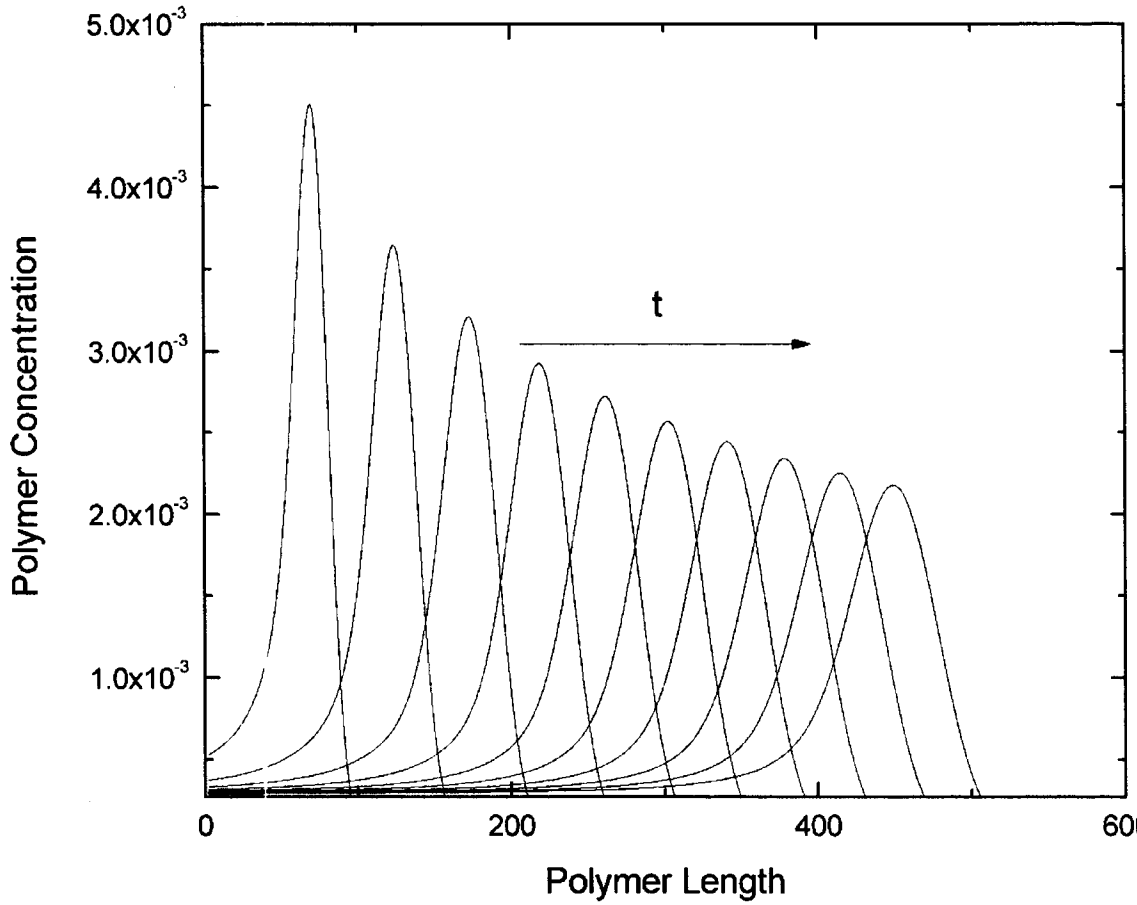

Figure3.2 Special case in which no polymer can escape. The growth front will decay to uniform small value. The following parameters are used: k_0=100, k_1=100, r_0=100, r_1=10, r_2=0, r_3=0.001, A_{out}=10, F_{out}=15, u_1=0.1, u_2=0

A special case is u_2=0, in which no polymer can escape from the system. Figure 3.2 shows how concentrations of different length polymer evolve with time. Because

polymers can neither escape from the system nor decompose to shorter ones, they can only keep growing forever. Hence there is no stationary state for the whole system in this condition. However, for any polymer with given length, it's still possible to converge to a fixed value, as long as its generation rate equals its consumption rate. In this case, Eq 3.10 is still correct and an be rewritten as:

$$\frac{r_1}{k_1}x^2-(r_1A^*+\frac{r_1}{k_1})x+r_1A^*=0$$

$$\Rightarrow(\frac{r_1}{k_1}x-r_1A^*)(x-1)=0$$

$$\Rightarrow x_1=k_1A^*;x_2=1$$

If x_1 is the solution, we have

$$-r_1A_nA^*+\frac{r_1}{k_1}A_{n+1}=0 \text{ and } r_1A_{n-1}A^*-\frac{r_1}{k_1}A_n=0$$

They mean that there is no polymer growing flux from length n-1 to n or n to n+1. If it's true, there will be no polymer growing to infinitely long, which is obviously wrong. Hence, the correct solution is x=1, e. g. all polymer will converge to the same concentration.

In this case, the behaviour of this system depends on the balance between polymer escape rate u_2 and polymerization rate r_1. When no polymer can escape from the system, all polymers will keep growing forever. With $u_2\neq0$, any given polymer will eventually escape from the system. Hence the system contains polymers of finite length. The faster the polymerization rate, the longer polymers can grow to before escape from the system.

Hence, an increment of polymerization of efficiency will indeed shift the equilibrium position of the system.

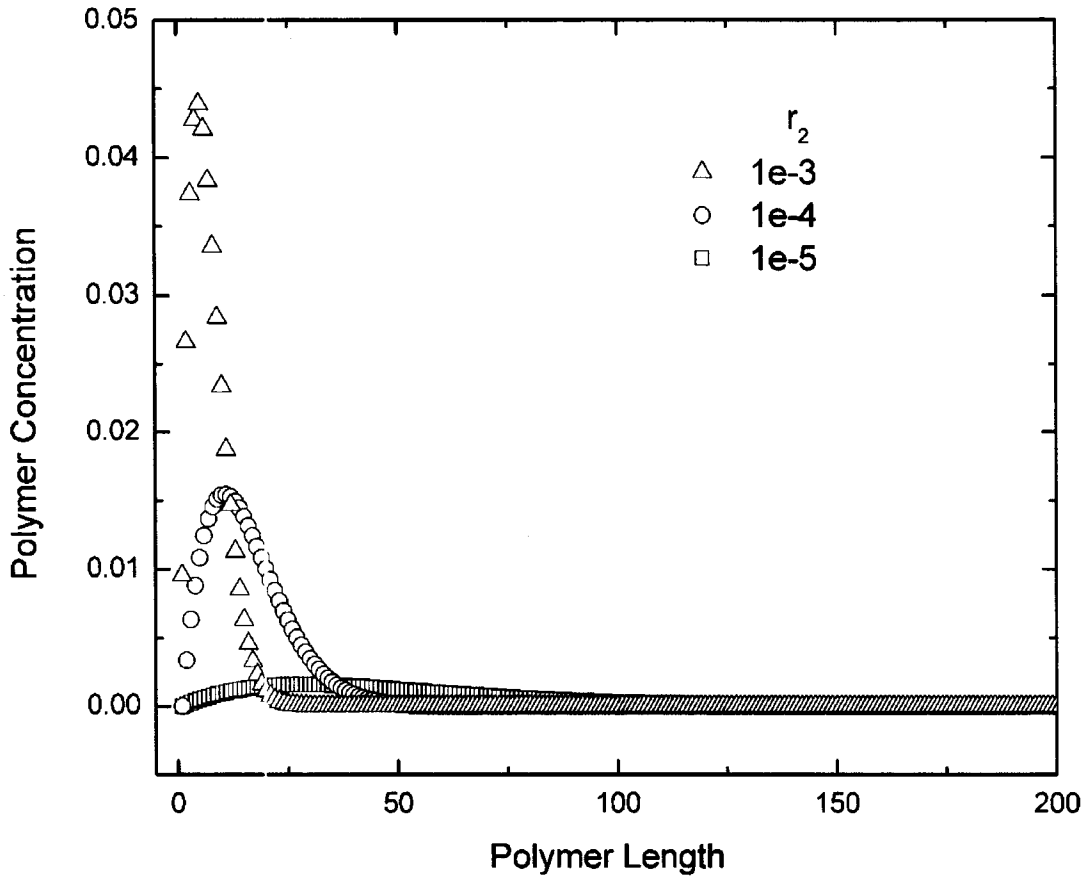

Figure 3.3 Stationary distributions of polymer concentrations as a function of length when polymer down rate $r_2 \neq 0$. Even when no polymer can escape from the system, the polymers can't grow to infinitely long. The following parameters are used: k_0=100, k_1=100, r_0=100, r_1=10, r_3=0.001, A_{out}=10, F_{out}=15, u_1=0.1, u_2=0

3.4.2 Results When Length is Limited by Polymer Breakdown

Decomposition is always a problem for polymers, and it's a big problem for RNA. Because polymers can split at any position of the chain, the longer the polymer is the higher the decomposition rate (r_2*(n-1)*A_n). Instead of growing to infinite length, long polymers will eventually break down to short polymer. On the other hand, with concen-

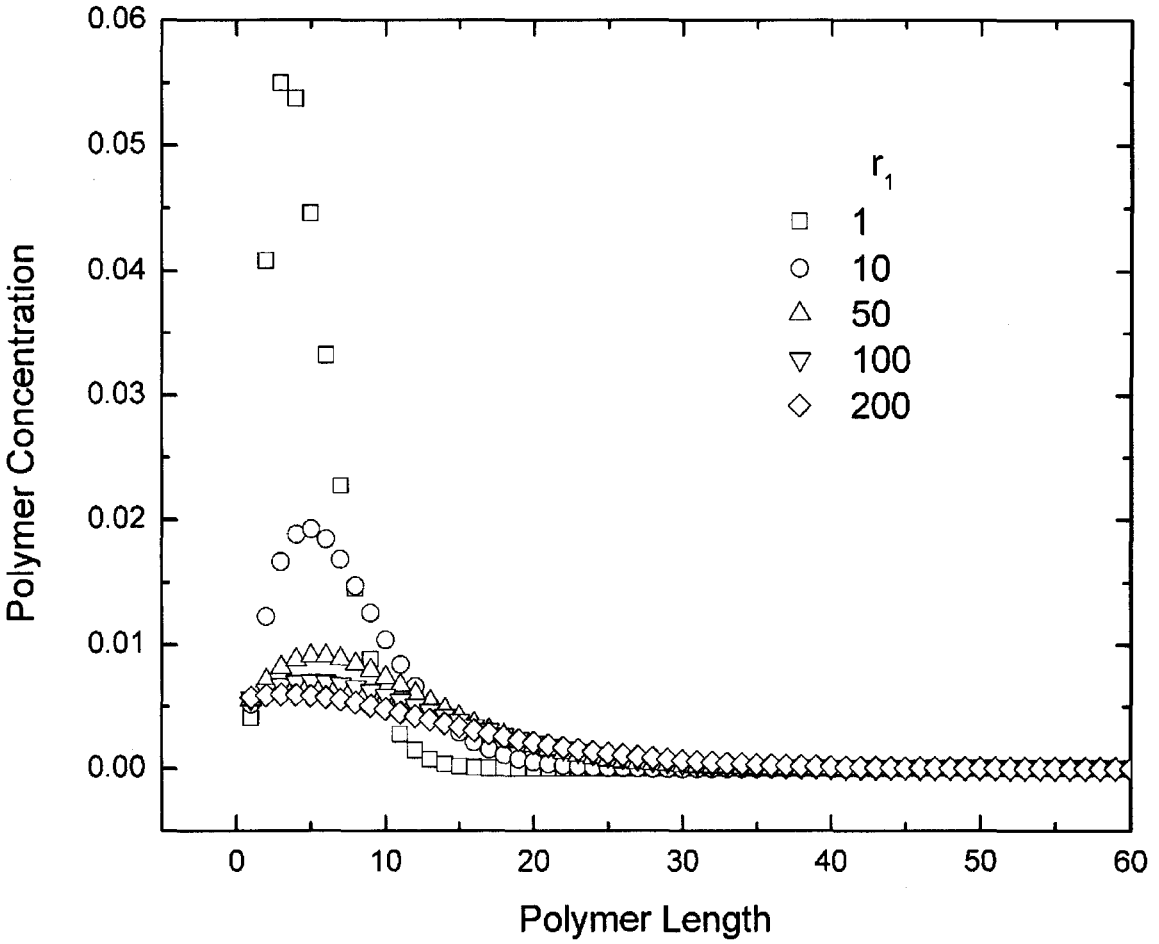

Figure 3.4 Stationary distributions of polymer concentrations as a function of length when u_2=0. The following parameters are used: k_0=100, k_1=100, r_0=100, r_2=0.001, r_3=0.001, A_{out}=10, F_{out}=15, u_1=0.1, u_2=0

tration increased by decomposition of long polymers, those short polymers will polymerize more long ones. When polymerization and decomposition rates come to balance, there will be a peak in the middle as shown in Fig 3.3. Hence, with the existence of polymer decomposition, the polymer length distribution will change a lot and it may also be true for the behaviour of the system, and therefore it is reasonable to take account of the effect of r_2. Obviously, the smaller the decomposition rate, the longer the polymers

can grow as shown in Fig. 3.3, which is good for the emergence of long functional polymers. However, to reduce the spontaneous break down rate, every single chain in all polymers need to be stabilized, which is essentially impossible for a few catalytic molecules. Hence, we won't vary the break down rate r_2 in the simulation. Meanwhile, polymer escape rate may change. Especially in the case of RNA enclosed in lipid vesicles, if the formation of lipid is also catalyzed by ribozyme in the vesicle, there may be feedback between the membrane permeability and RNA distributions.

Changing r_1 and u_2, we obtain Figures 3.5-3.8. Similar to the non-decomposition case, faster polymerization rate can channel material towards longer polymers, and the average polymer length and maximum length of polymers is positively related to polymerization rate r_1. However, when r_1 comes close to monomer activation rate r_0, all activated monomers are used up by polymerization reaction. Hence further increment of r_1 won't change the behaviour of the system too much.

When the effect of u_2 is taken under investigation, there are several interesting phenomenon occur. Firstly, if we look at total monomers concentration M within the system, no matter in the form of monomer or polymer, we found that for a given polymer escape rate u_2, it will converge to a constant. This result can be explained as follows. When equilibrium of this system is reached, the number of monomers diffusing into this system must equal to the number of monomers escaping from this system in the form of polymer. Hence,

$$u_1(A_{out} - A_1) = u_2 \sum_{n>1} n \cdot A_n \Rightarrow u_1 A_{out} = u_2 \sum_{n} n \cdot A_n + (u_1 - u_2) A_1 \qquad (3.14)$$

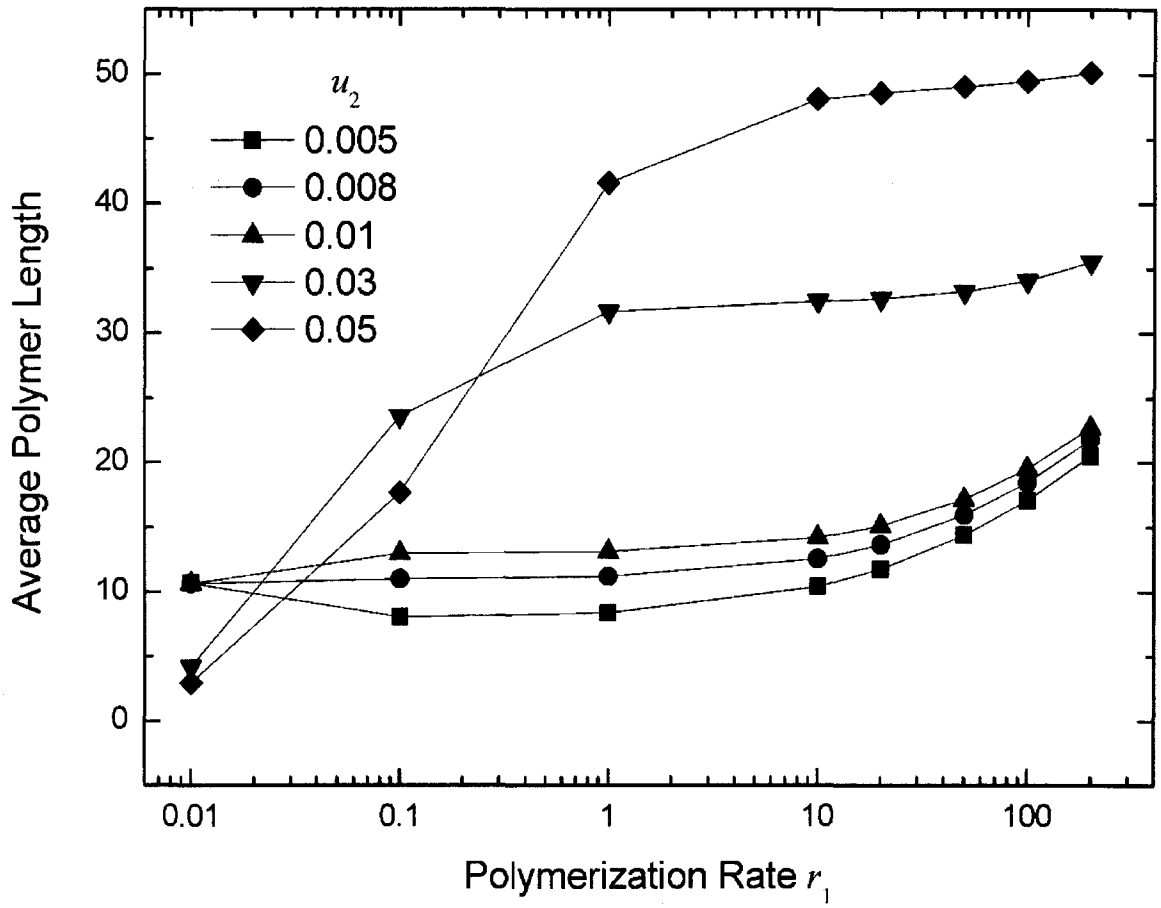

Figure 3.5 Average polymer length as a function of polymerization rate. The following parameters are used: k_0=100, k_1=100, r_0=100, r_2=0.001, r_3=0.001, A_{out}=10, F_{out}=15, u_1=0.1

When $r_0>>r_1>>r_2$, almost all monomers are activated and catalyzed to polymer form. Hence, $(u_1-u_2)A_1$ is a small term compared to M, and can be omitted in this case. We obtain

$$u_1 A_{out} = u_2 \sum_n n \cdot A_n = u_2 M \tag{3.15}$$

$u_1 * A_{out}$ is constant, hence when u_2 is fixed, total monomer in the system won't change, and it will decrease with an increasing u_2 as shown in simulation result

When polymer can escape from the cell, products of polymerization are removed from the system. Hence we can expect the equilibrium will shift towards longer polymers

for a larger u_2, which means a bigger average polymer length. Its negative effect is that much less material left in the system. And when u_2=1, no polymer stay in the system, the cell become a tube. The above conclusion can also be obtained by analysis the equations.

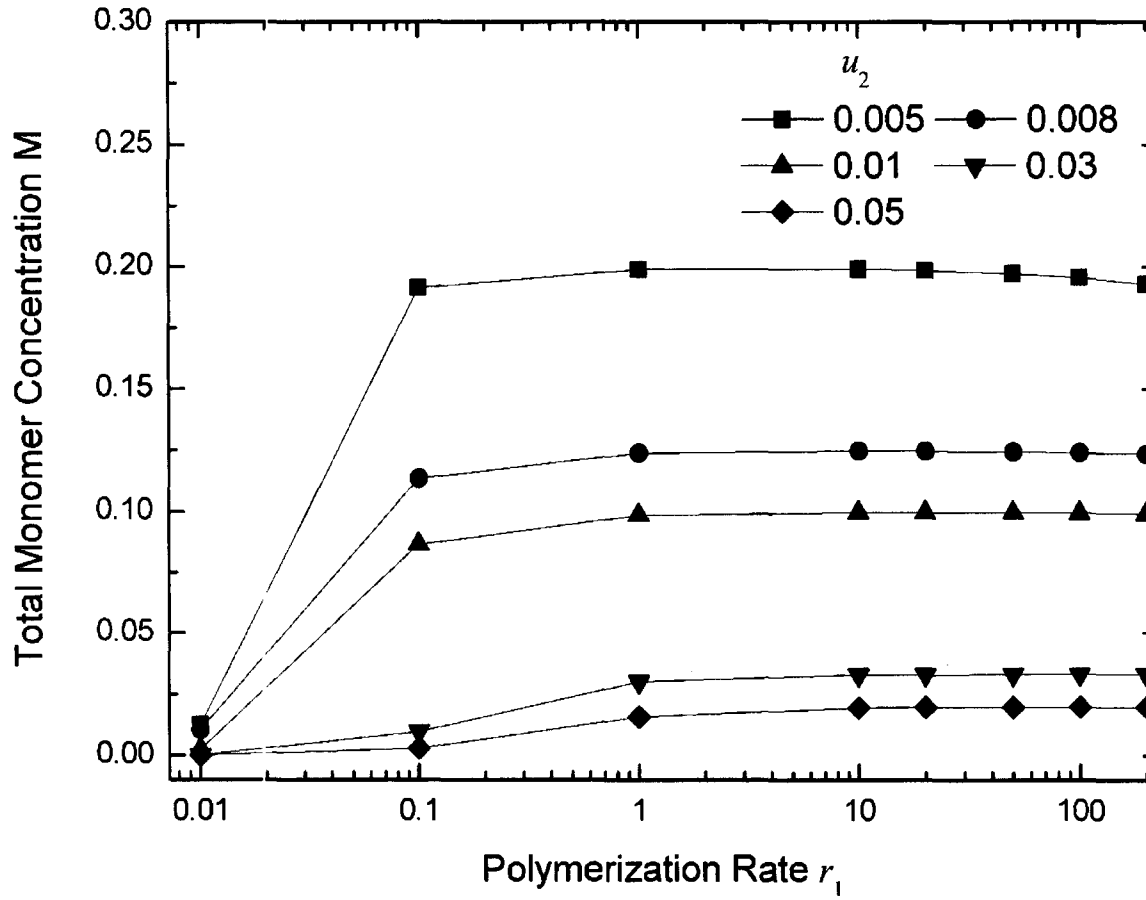

Figure 3.6 Total monomer concentration M as a function of polymerization rate. The following parameters are used: k_0=100, k_1=100, r_0=100, r_2=0.001, r_3=0.001, A_{out}=10, F_{out}=15, u_1=0.1

Sum over Eq. 3.8 for all polymers at equilibrium

$$\Rightarrow 0 = -u_2 \sum_n A_n + r_1 A_1 A^* - \sum_n r_2 (n-1) A_n + \sum_n \sum_{m>n} 2 r_2 A_m$$

$$\Rightarrow 0 = -u_2 \sum_n A_n + r_1 A_1 A^* - \sum_n r_2 (n-1) A_n + \sum_n 2 r_2 (n-2) A_n$$

$$\Rightarrow u_2 \sum_n A_n = r_1 A_1 A^* + \sum_n r_2 (n-3) A_n \tag{3.16}$$

Left side of Eq. 3.16 means rate of polymers escaping from the cell. The first term of right side of the equation means newly formed polymers by polymerizing monomer, and the second term means newly formed polymers by decomposition. The whole equation means at equilibrium, formation rate of polymers equals their escaping rate. If the term related with monomer is negligible, which is true for a fast activation rate when almost all monomers are activated, we can obtain

$$\Rightarrow (u_2 + 3r_2) \sum_n A_n = \sum_n r_2 \cdot n \cdot A_n$$

$$\Rightarrow average\ size\ of\ polymers\ \bar{A} = \frac{\sum_n n \cdot A}{\sum A_n} = \frac{u_2}{r_2} + 3 \tag{3.17}$$

Hence, the average polymer length of polymers is positively related to polymer escaping rate u_2, and negatively related to polymer breakdown rate r_2. The assumption that the term related with monomer is negligible is true only when r_1 is big, which means that a fast polymerization rate consumes all monomers and activated monomers. It's proved qualitatively that average size of polymer is positively correlated with u_2 as in Fig. 3.5, but the quantitative expression of Eq 3.17 works not so well. More investigation is needed.

If we look at the effect of u_2 on polymers of different length, an intuitive guess will tell us that no matter the length of polymer, the larger the escape rate, the smaller the number of polymers stay in the system, even there are relative concentration change between different polymers. However, the simulation tells us something different. When calculating the concentration of short polymers, say shorter than 50 and those longer than

50, we found totally opposite response to u_2: the concentration of shorter ones decreases as we predicted, but that of longer ones increases firstly and then decreases as shown in Fig. 3.7 and 3.8. It may mean that the concentration of short polymers is negatively correlated with u_2, and the concentration of long polymers is positively correlated with u_2. While the left part of Fig. 3.8 tells the same story as about long polymers, the right part shows the shift of balance between long polymers and short polymers. After all, 50 is an arbitrary chosen criteria for long polymer. It's possible that the concentration of polymers much longer than 50 is positively correlated with u_2, while that of shorter ones is a negative correlation.

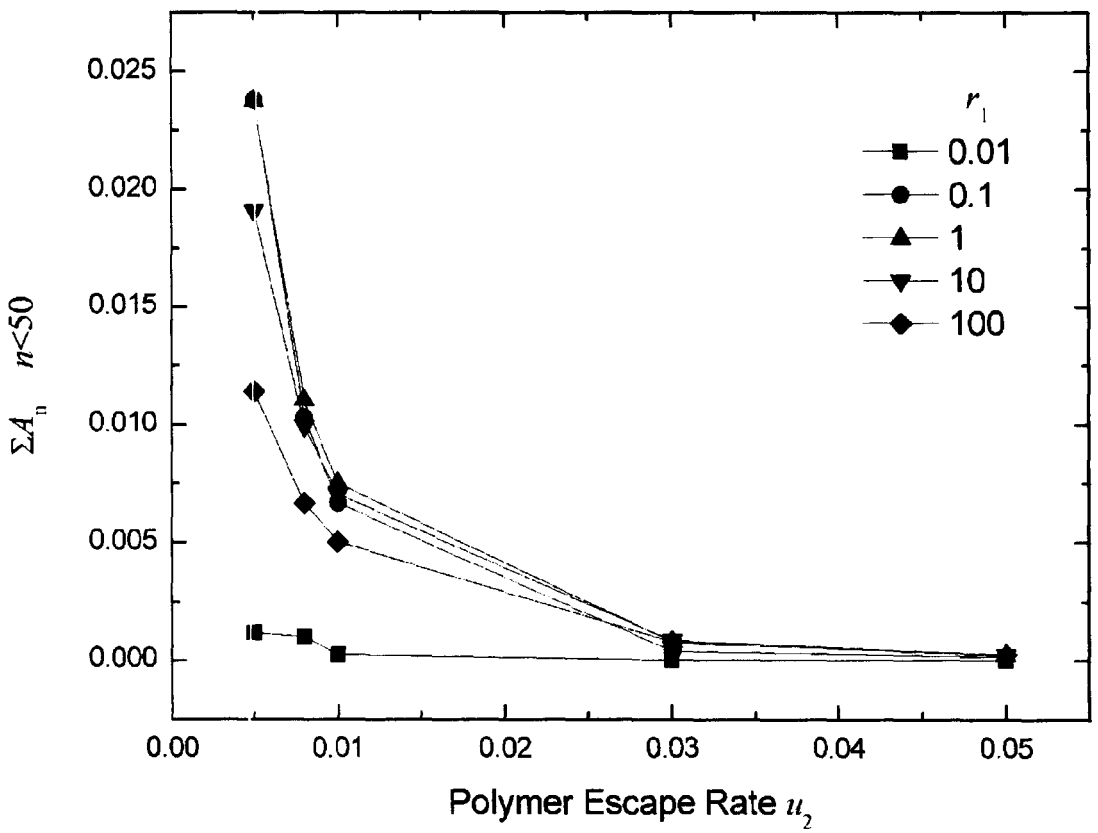

Figure 3.7 Total concentration of polymer shorter than 50 as a function of polymer escape rate. The following parameters are used: k_0=100, k_1=100, r_0=100, r_2=0.001, r_3=0.001, A_{out}=10, F_{out}=15, u_1=0.1

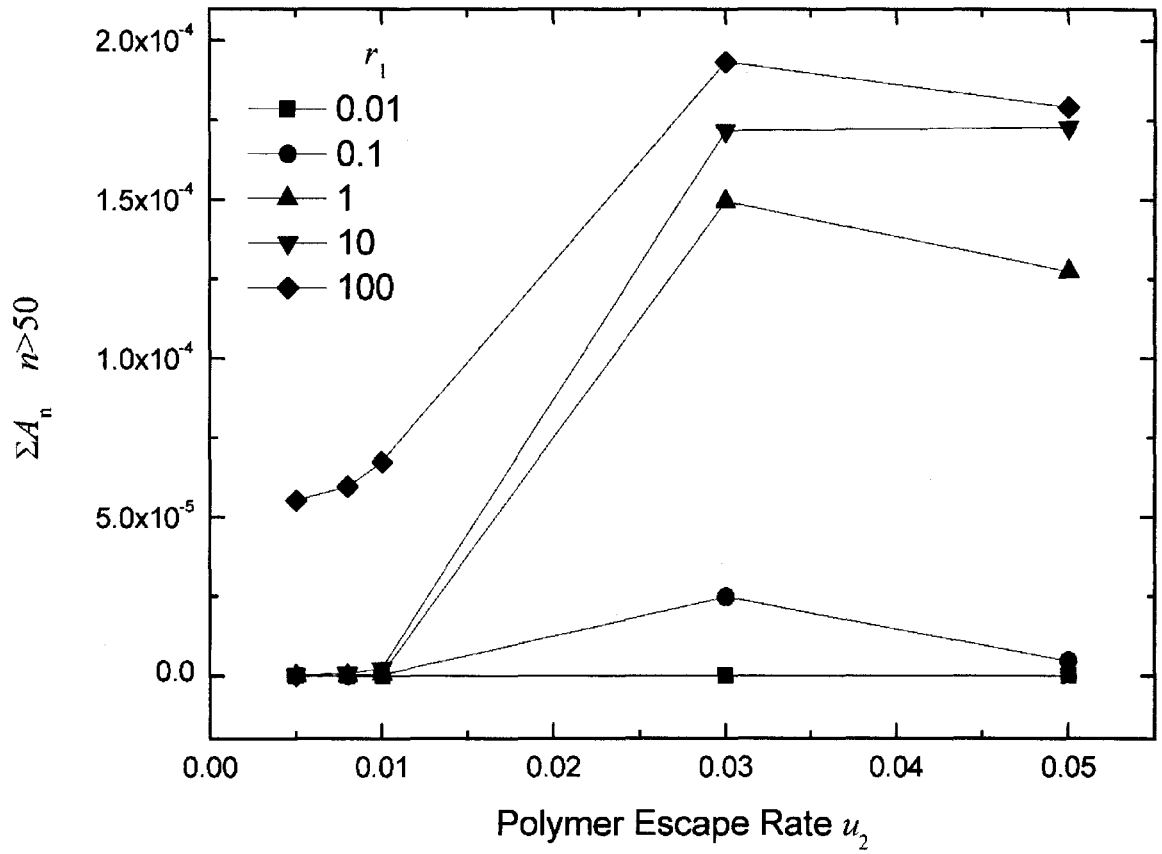

Figure 3.8 Total concentration of polymer longer than 50 as a function of polymer escape rate. The following parameters are used: k_0=100, k_1=100, r_0=100, r_2=0.001, r_3=0.001, A_{out}=10, F_{out}=15, u_1=0.1

3.5 Conclusions

The polymerization rate r_1 can indeed change the system equilibrium towards longer polymers under all these conditions. But there also exists an upper limit of the improvement, which I think depends on the availability of monomers and binding site on polymers. With the increasing of r_1, average polymer length become longer, and monomers and binding site became lesser. Hence the further increase of r_1 may be not so efficient to shift the distribution of polymers.

Polymer decomposition rate r_2 can change the behaviour of system dramatically. However, it's easy to find a catalyst to increase the decomposition speed, but it's quite hard to produce enough molecules to stabilize every single chain of all polymers. Only at later stage of life, small number of important polymer produced on demand by template directed replication or translation can be stabilized. Hence, it's not the parameter we can try to improve at early stage of life. We can only try to prove that the spontaneous polymer decomposition rate r_2 won't make the evolution impossible for our theory.

From above sections, we know that a permeable membrane may not be a bad thing. Otherwise longer polymers are harder to form. At later stage of evolution in which some rare long polymers matter a lot, a semi permeable membrane may be better for the system.

3.6 Future Work

One immediate step for future research is to considerate feedback by catalysis. Monomer activation rate r_0 is the speed limiting step while polymerization rate r_1 can shift the equilibrium distribution. Both can be accelerated by catalysts. Considering the potential ability of RNA as catalyst, we can assume that a small fraction of polymers longer than a minimum (say n = 100) can act as activation catalysts or polymerization catalysts. These catalysts can not only catalyze the formation of themselves directly or indirectly, but also help the formation of new longer polymers, which can be even better catalyst. Whether a polymerization system like this will evolve to more and more complex system leading to the first life, or can only stay as a bunch of long polymers

depends on the balance between the possibility of polymer acting as polymerization or activation catalyst and the efficiency of these catalysts at a given length.

Another approach for future research will be investigation of sequence polymerization from more than one type of monomers, such as 4 for RNA. It will then be necessary to keep track of the concentration of each sequence of a given length. Sequence will introduce much more types of polymers for a given length. With only universal polymerization catalyst, the monomers and energy will be easily wasted into exponentially growing types of useless sequences before the emergence of more efficient catalyst. Hence, specific catalysts are needed to channel limited resource into really useful polymerizations. In this case, the effect of auto-catalytic network for this system is worth consideration. Furthermore, the possibility of spontaneous emergence of template-directed polymerization from this system also needs to be investigated.

The long catalytic polymers formed by this kind of feedback, will exist in small quantities and be subject to stochastic effect. For example, several highly efficient polymerase sequences may greatly shift the equilibrium towards longer polymers, but these catalysts can be lost by diffusion out of system randomly, which will cause the system fall back to shorter polymers. For an autocatalytic network formed by feedback between these polymers, random drift may be important. The disappearance of crucial reactant or catalyst may cause the collapse of the whole network. The emergence of a new catalyst or reactant may lead to a new pathway which can change the structure of the network. Hence, it may be better to use a stochastic method such as Monte Carlo method or molecular dynamics to treat this kind of system.

BIBLIOGRAPHY

Bachmann PA, Luisi PL, Lang J (1992) Autocatalytic self-replicating micelles as models for prebiotic structures. *Nature* 357: 57-59.

Bagley RJ, Farmer JD (1991) Spontaneous emergence of a metabolism. In *Artificial Life II*, Santa Fe Institute Studies in the Science of Complexity. Eds. Langton CG, Taylor C, Farmer JD, Rasmussen S.

Bartel DP, Unrau PJ (1999) Constructing an RNA World. *Trends Biochem. Sci.* 24: M9-M13.

Bozic B, Svetina S (2004) A relationship between membrane properties forms the basis of a selectivity mechanism for vesicle reproduction. *Eur. Biophys. J.* 33: 565-571.

Bradford JA, Dill KA (2007) Stochastic innovation as a mechanism by which catalysts might self-assemble into chemical reaction networks. *Proc. Nat. Acad. Sci. USA* 104: 10098-10103.

Clark BC (2001) Planetary interchange of bioactive material: probability factors and implications. *Orig. Life. Evol. Biosph.* 31:185 - 197

Copley S.D., Smith E., Morowitz H.J. (2007), The origin of the RNA world: Co-evolution of genes and metabolism, *Bioorganic Chemistry*, 35:430-443

Dalrymple, G.B. (1991). *The Age of the Earth.* California: Stanford University Press.

Dyson FJ (1985) *Origins of life.* Cambridge University Press, New York.

Ewens WJ (2004) *Mathematical Population Genetics: theoretical introduction.* Springer, New York.

Farmer JD, Kauffman SA, Packard NH (1986) Autocatalytic replication of polymers. *Physica D* 22: 50-67.

Fellerman H, Solé RV (2007) Minimal model of self-replicating nanocells: a physically-embodied, information-free scenario. *Phil. Trans. R. Soc. B* 362: 1803-1811.

Ferris J.P., Hill A.R., Liu R. and Orgel L.E. (1996), Synthesis of long prebiotic oligomers on mineral surfaces, *Nature* 381 : 59–61.

Ferris J.P.(2002), Montmorillonite catalysis of 30–50 mer oligonucleotides: laboratory demonstration of potential steps in the origin of the RNA World, *Orig. Life Evol. Biosph.* 32 : 311–332

Ganti T (1979) *A theory of biochemical supersystems and its application to problems of natural and artificial biogenesis.* University Park Press, Baltimore, Maryland.

Gilbert W. (1986) Origins of Life – The RNA World. *Nature* 319:618-618.

Goldstein RA (2006) Emergent robustness in competition between autocatalytic chemical networks. *Orig. Life. Evol. Biosph.* 36: 381-389.

Haldane, JBS (1929). The origin of life. *Rationalist Annual* 1929:148-69

Hancyk MM, Szostak JW (2004) Replicating vesicles as models of primitive cell growth and division. *Curr. Op. Chem. Biol.* 8: 660-664.

Higgs PG, Pudritz RE. (2007) From protoplanetary disks to prebiotic amino acids and the origin of the genetic code. In *Planetary systems and the origins of life*, Cambridge

Series in Astrobiology, vol 3. Eds. Pudritz RE, Higgs PG. Stone J. Cambridge University Press.

Hoyle F, Wickramasinghe NC (1999) Comets—a vehicle for panspermia. *Astrophys Planet Sci* 268:333 - 341

Hunding A, Kepes F, Lancet D, Minsky A, Norris V, Raine D, Sriram K, Root-Bernstein R(2006), Compositional complementarity and prebiotic ecology in the origin of life, *Bioessays,* 28: 399-412

Inoue T, Orgel LE (1983) A nonenzymatic RNA polymerase model. *Science* 219:859 - 862

Jeffares DC, Poole AM, Penny D (1998) Relics from the RNA world. *J. Mol. Evol.* 46: 18-36.

Johnston WK, Unrau PJ, Lawrence MS, Glasner ME, Bartel DP (2001) RNA-catalyzed RNA polymerization: Accurate and general RNA-templated primer extension. *Science.* 292: 1319-1325.

Joyce GF (2002) The antiquity of RNA-based evolution. *Nature* 418: 214-221.

Karlin S, McGregor J (1962) On a genetics model of Moran. *Proc. Camb. Phil. Soc.* 58: 299-311.

Kauffman SA (1986) Autocatalytic sets of proteins. *J. theor. Biol.* 119:1-24.

Kauffman SA (1993) *Origins of Order.* Oxford University Press.

Kazakov S, Altman S (1992) A trinucleotide can promote metal ion-dependent specific cleavage ofRNA. *Proc Natl Acad Sci USA* 89:7939 - 7943

Kazakov SA (1996) Nucleic acid binding and catalysis by metal ions. In: Hecht SM (ed) *Bioorganic chemistry: Nucleic acids*. Oxford University Press, New York, pp 244 - 287, 467 - 476

Luisi PL, Walde P, Oberholzer T. (1999) Lipid vesicles as possible intermediates in the origin of life. *Curr. Op. Coll. Int. Sci.* 4:33-39.

Luisi PL, Ferri F, Stano P (2006) Approaches to semi-synthetic minimal cells: a review. *Naturwissenschaften* 93: 1-13.

Lunine JI. (2005) *Astrobiology – A Multidisciplinary Approach.* San Francisco: Addison Wesley.

Macia J, Solé RV. (2007) Protocell reproduction in a spatially extended metabolism-vesicle system. *J. Theor. Biol* 245: 400-410.

Maxwell ES, Fournier MJ (1995) The small nucleolar RNAs. *Annu Rev Biochem* 35:897-934

Miller SL (1953). Production of Amino Acids Under Possible Primitive Earth Conditions. *Science* 117: 528

Mojzsis SJ, Arrhenius G, Mckeegan KD, Harrison TM, Nutman AP Friend CRL (1996). Evidence for life on Earth before 3800 million years ago. *Nature* 384:55-59

Monnard PA, Luptak A, Deamer DW (2007) Models of primitive cellular life: polymerases and templates in liposomes. *Phil. Trans. R. Soc. B* 362: 1741-1750.

Moran PAP (1958) Random processes in genetics. *Proc. Camb. Phil. Soc.* 54: 60-71.

Morbidelli A (2007). Impacts in the primordial history of terrestrial planets, *Comptes rendus. Geoscience* 339:907-916

Oparin, AI (1929), *The origin of life*, Moskovskiy Rabochiy, Moscow

Orgel LE (1998) Polymerization on the rocks: theoretical introduction. *Orig Life Evol Biosphere* 28:227 - 234

Orgel LE (2004) Prebiotic chemistry and the origin of the RNA world. *Crit. Rev. Biochem. Mol. Biol.* 39:99-123.

Press WH, Flannery BP, Teukolsky SA, Vetterling WT (1992) *Numerical recipes in C : the art of scientific computing.* 2ed. Cambridge University Press

Pohorille A, Deamer D (2002) Artificial cells: prospects for biotechnology. *Trends in Biotech.* 20: 123-128

Rajamani S., Vlassov A., Benner S., Coombs A., Olasagasti F., Deamer D. (2008), Lipid-assisted synthesis of RNA-like Polymers from mononucleotides. *Orig Life Evol Biosph* 38: 57-74

Schopf JW (1993) Microfossils of the early archean apex chert – New evidence of the antiquity of life. *Science* 260:640-646

Segré D, Lancet D, Kedem O, Pilpel Y (1998) Graded auutocatalysis replication domain (GARD): kinetic analysis of self-replication in autocatalytic sets. *Orig Life Evol. Biosph.* 28: 510-514.

Segré D, Ben-Eli D, Lancet D (2000) Compositional genomes: Prebiotic information transfer in mutually catalytic noncovalent assemblies. *Proc. Nat. Acad. Sci. USA* 97: 4112-4117.

Segré D, Shenhav B, Kafri R, Lancet D (2001a) The molecular roots of compositional inheritance. *J. theor. Biol.* 213: 481-491.

Segré D, Ben-Eli D, Deamer DW, Lancet D (2001b). The lipid world. *Orig Life Evol. Biosph.* 31: 119-145.

Seifert U, Berndl K, Lipowski R (1991) Shape transformations of vesicles: Phase diagram for spontaneous curvature and bilayer-coupling models. *Phys. Rev. A* 44: 1182-1202.

Shapiro R. (1988) Prebiotic ribose synthesis – a critical review. *Orig Life Evol. Biosph.* 18:71-85.

Shapiro R. (2006) Small molecule interactions were central to the origin of life. *Quart. Rev. Biol.* 81: 105-125.

Shenhav B, Oz A, Lancet D. (2007) Coevolution of compositional protocells and their environment. *Phil. Trans. R. Soc. B* 362: 1813-1819.

Sleeper H. L. and Orgel L. E. (1979) The catalysis of nucleotide polymerization by compounds of divalent lead. *J. Mol. Evol.* 12: 357–364

Solé RV, Munteanu A, Rodriguez-Caso C, Macia J. (2007) Synthetic protocell biology: from reproduction to computation. *Phil. Trans. R. Soc. B* 362: 1727-1739.

Stribling, R. & Miller, S. L. (1987) Energy yields for hydrogen cyanide and formaldehyde syntheses: the HCN and amino acid concentrations in the primitive ocean. *Orig. Life Evol. Biosph.* 17, 261–273.

Szabo P, Scheuring I, Czaran T, Szathmary E. (2002) In silico simulations reveal that replicators with limited dispersal evolve towards higher efficiency and fidelity. *Nature* 420: 340-343.

Szathmary E, Santos M, Fernando C (2005) Evolutionary potential and requirements for minimal protocells. *Top. Curr. Chem.* 259: 167-211.

Tepfer D, Leach S (2006) Plant seeds as model vectors for the transfer of life through space. *Astrophys Space Sci* 306:69 - 75

Walde P (2006) Surfactant assemblies and their various possible roles for the origin of life. *Orig. Life Evol. Biosph.* 36: 109-150.

Yeomans JM (1992) *Statistical Mechanics of Phase Transitions.* Oxford University Press.

Zaher HS, Unrau PJ (2007) Selection of an improved RNA polymerase with superior extension and fidelity. *RNA* 13: 1017-1026.